Final report

1. Project details

Project title	IEA PVT task participation
File no.	64017-05157
Name of the funding scheme	EUDP
Project managing company / institution	DTU Byg, Danmarks Tekniske Universitet
CVR number (central business register)	30060946
Project partners	RACELL
Submission date	22/12-2020

Authors: Janne Dragsted (DTU), Simon Furbo (DTU), Mark Dannemand (DTU), Bengt Perers (DTU), Ioannis Sifnaios (DTU), Adam R. Jensen (DTU), Yakov Safir (RACELL)

2. Summary

The purpose of the project is to be the Danish participant in the IEA (International Energy Agency) SHC (Solar Heating & Cooling) programme task 60 project on Photovoltaic thermal collector, PVT systems: ”Application of PVT Collectors”, which provides an overview on the present state-of-the-art of the PVT technology world-wide.

PVT panels can produce heat, electricity and cooling for buildings. Due to the complex interaction between the different components of PVT systems and buildings, there are many different designs of PVT systems and it is not easy to optimize the design of PVT systems.

A demonstration PVT/heat pump system with PVT panels produced by RACELL Technologies has been tested in the laboratory test facilities at the Department of Civil Engineering, Technical University of Denmark. The PVT panels were connected to a heating system consisting of two storage tanks and a heat pump. A TRNSYS simulation model of the system has been developed and validated by means of measurements from the tested system. Calculations with the validated model elucidated how best to design the system.

Experimental investigations on roof mounted PVT panels and vertical façade integrated PVT panels have been carried out to elucidate their performances in real weather conditions. The measured performances were compared to calculated performances using a simulation model.

Furthermore, measurements of performances of full scale PVT systems in buildings at different locations in Denmark were analysed.

The results of the project were presented at an international information meeting for all interested at the Technical University of Denmark. Both presentation by Danish and international experts in the field were given. The project results forms a good basis for further development of PVT panels and PVT systems.

Formålet med projektet er dansk deltagelse i IEA (International Energy Agency) SHC (Solar Heating & Cooling) programme task 60 projektet vedrørende Photovoltaic thermal collector, PVT anlæg: "Application of PVT Collectors". Det international projekt skaber et verdensomfattende overblik over PVT området og netværk inden for PVT området.

PVT paneler kan producere varme, elektricitet og køling til bygninger. På grund af det komplekse samspil mellem de forskellige komponenter af PVT anlæg og bygninger er der mange forskellige udformninger af PVT anlæg og det er vanskeligt at bestemme optimale anlægsudformninger.

Et demonstrationsanlæg med PVT paneler (hybrid solcelle og termisk solfanger) produceret af RACELL Technologies er afprøvet i en prøvestand på DTU Bygs forsøgsareal. PVT panelerne er koblet til et varmeanlæg bestående af to lagertanke og en varmepumpe. Der er udviklet en TRNSYS simuleringsmodel af det afprøvede anlæg, og simuleringsmodellen er valideret ved hjælp af målinger for det afprøvede anlæg. Der er gennemført beregninger for at klarlægge hvorledes anlægget bedst udformes.

Eksperimentelle undersøgelser af PVT paneler placeret på tagflader og lodret placerede facadeintegrerede PVT paneler er gennemført for at klarlægge panelernes ydelser under virkelige vejrforhold. De målte ydelser er sammenlignet med ydelser beregnet med en simuleringsmodel.

Derudover er målinger for fuldskala PVT anlæg i bygninger forskellige steder i Danmark analyseret.

Projektets resultater blev præsenteret på et informationsmøde for alle interesserede på Danmarks Tekniske Universitet. Mødet inkluderede præsentationer af danske og internationale eksperter. Projektets resultater udgør et udmærket grundlag for videreudvikling af PVT paneler og PVT anlæg.

3. Project objectives

The objective of the project was, through participation in the international IEA Task 60 project Application of PVT Collectors, to provide an overview of the state of the art of PVT technology. Further, simulation models both for the performance of PV panels and for a PVT/heat pump system were developed and validated by means of measurements for PVT panels and for the PVT/heat pump system.

The project had the following work packages (WPs) and milestones:

WP 1 – Analyses of measurements from a PVT/heat pump system. Detailed analyses of the measurements of the performance of a laboratory system tested in the research test facility of Department of Civil Engineering, Technical University of Denmark were carried out. The measuring period had a duration of one year. The first project milestone M1, Detailed analyses of measurements for a PVT/heat pump system was achieved as planned by means of a paper published in a scientific journal.

WP 2 – Cooling investigations. Laboratory experiments on PVT panels ability to cool the fluid passing through the panel during nights have been carried out. The cooling is based on the infra-red radiation from the panel to the cold night sky. Further, the extra electricity production of the PVT panel caused by cooling of the panel

during sunny periods has been elucidated. The second milestone of the project M2, Experimental investigations of the cooling ability of PVT panels was achieved and the results are presented in section 5.

WP 3.1 – Efficiency of PVT panels. Laboratory tests of PVT panels have been carried out with the aim to characterize the performances of the panels. The tests were carried out according to international standards on PVT panels and efficiency expressions were determined. Among other things, the influence of the panel temperature and the wind velocity on the efficiencies was elucidated. The third milestone of the project, M3.1, characterization of PVT panel was achieved and the results are presented in section 5.

WP 3.2 – Characterization of PVT panel integrated in concrete facade. Laboratory tests have been carried out for a PVT panel integrated in a concrete wall. Measurements have elucidated how the weather and panel temperature influence the performance and the construction. The milestone M3.2, Characterization of PVT façade was achieved by means of a conference paper.

WP 4.1 – Simulation model of a PVT/heat pump system. A TRNSYS simulation model of the PVT/heat pump system investigated in WP 1 was developed and validated by means of the measurements from the demonstration system. The milestone M4.1, Simulation model of PVT/heat pump system developed and validated was achieved by means of a scientific paper.

WP 4.2 – Simulation model of PVT panel integrated in concrete façade. A simulation model of a PVT panel integrated in a concrete wall was developed. The thermal mass of the concrete wall is considered in the model. The milestone M4.2, Simulation model of a PVT façade developed and validated was achieved as planned.

WP 5 – Theoretical optimization of PVT/heat pump systems. Performances of differently designed PVT/heat pump systems have been calculated with the validated simulation model. Based on the calculations optimal system designs have been determined. The milestone M5, Optimal systems for buildings with different heating and cooling demand was achieved by means of a paper published in a scientific journal.

WP 6 – Analyses of operation of full scale PVT systems. Analyses of measurements for a full scale PVT system in practice have been carried out in order to elucidate the performances, to gain experience from practice and to elucidate possible improved system designs. A simulation model for the system was developed and validated by means of measurements. The milestone M6, operation and performance of full scale system documented was achieved as planned.

WP 7 – Participation in IEA meetings. The project results were presented at the IEA Task 60 expert meetings. All the meetings were attended including the online meetings. One of the expert meetings was organized at the Technical University of Denmark in Kgs. Lyngby in October 2019.

WP 8 – Dissemination. A paper on the TRNSYS simulation model of PVT/heat pump systems was published in a scientific journal and a paper focused on characterization of PVT panels integrated in concrete facades was presented at a conference. Further, an information meeting with Danish and international experts presenting the state of art of the PVT technology was organized for the Danish solar industry at the Technical University of Denmark in October 2019.

The project was carried out as originally planned and all the planned milestones were achieved within the project period. The risks of the project were related to errors on components and measuring equipment, to missing simulation components in TRNSYS and to slow review process of scientific papers. All the risks were overcome by means of thorough checks of the components of the PVT systems, the PVT panels and the measuring equipment in the very start of the test periods, by experienced and skilled researchers carrying out the simulation work and by preparing the scientific papers early in the project period.

4. Project implementation

The project was executed according to the original plan, with participation in all of the activities mentioned in the project description and delivery of the specified milestones. The project was only slightly affected by the covid-19 pandemic, primarily that the two expert meetings in 2020 were held virtually instead of in person.

The risks of the project were related to errors on components and measuring equipment, to missing components in TRNSYS and to slow review process of scientific papers. All the risks were overcome by means of thorough checks of the components of the PVT systems, the PVT panels and the measuring equipment in the very start of the test periods, by experienced and skilled researchers carrying out the simulation work and by preparing the scientific papers early in the project period.

All the milestones of the project were achieved within the project period. Two of the milestones were however achieved somewhat later than originally planned. The project did not experience unexpected problems.

5. Project results

The original objectives of the project were obtained. Differently designed and installed PVT panels were characterized, the suitability of differently designed PVT systems were elucidated and simulation models which can be used to optimize the design of PVT panels and PVT systems were developed and validated. The project results are useful for manufacturers of solar collectors, PV panels and PVT panels in connection with their efforts to improve their products. The project results are also useful for consultants and planners aiming to improve marketed solar energy systems. Further, the project results are useful for solar energy researchers aiming to determine optimal solar energy systems for the future. Overall, the project results form an excellent basis for future development of solar energy solutions. The investigations of the project inclusive the project results are described in the sections 5.1-5.5 and section 5.6 describes how the project has been disseminated.

5.1 PVT/heat pump systems. Analyses of measurements, simulation model and system optimization

A PVT system was installed in the laboratory solar heating test facilities of the Technical University of Denmark. It consisted of an uninsulated PVT panel from RACELL with an absorber gross collector area of 3.1 m^2, with the PV cells covering 2.58 m^2 of the panel, see figure 1. The PVT collectors faced due south with a tilt of 45°. The PVT panel was installed with a distance of approximately 10 cm above the roof structure so that air could pass underneath it as well. The PV cell efficiency was nominally 18 % at STC (25ºC and 1000 W/m^2 and AM 1.5). The cells have an efficiency reduction of 0.4% per K above 25ºC. An AEconversion micro-inverter INV350-60 was installed between the PVT and the connection to the grid.

Figure 1. PVT panel installed at roof facing south with a tilt angle of 45º.

The thermal absorber of the PVT panel was connected in a solar collector loop to a heat exchanger spiral in the bottom of a 160 litres DHW storage tank. The hydraulic loop was also connected to a 200 litres “cold” buffer storage tank via a direct inlet to the tank. The solar collector loop and the cold storage tank contained a 40% glycol/water mixture. The storage tanks were located in an indoor test facility together with the heat pump, see figure 2. A sketch of the tested PVT/heat pump system with sensor locations and control strategy of the thermal part of the system is shown in figure 3.

Figure 2. DHW and cold storage tanks and heat pump in indoor test facility.

As the PVT panels were uninsulated and could work as heat exchangers with the ambient, they could still extract low temperature heat from the ambient, when no solar radiation was available.

Automated draw offs of hot water were made three times per day to simulate an actual installation in a house. 1.5 kWh of energy was tapped three times per day at 7 am, at noon and at 6 pm. This corresponds to three times approximately 45 litres of water at 48-51°C when the cold-water inlet temperature was 18-20°C. In some months, the tapped energy was down to 1.1 kWh per tapping due to clogged filters in the tapping loop, which caused a reduced flow rate during the tapping.

A Vølund F1155-6 heat pump was used to heat the DHW tank when the heat from the solar collectors was insufficient to maintain the required temperature level. This heat pump was designed to cover both a space heating and domestic hot water demand. The tested system was only used for domestic hot water, DHW supply. The heat pump was therefore a bit oversized.

A cold buffer storage tank was used as the source for the cold side of the heat pump. The thermal absorber of the PVT panels could charge both tanks. When high temperature heat was generated in the PVT panel, it was transferred to the DHW tank and when the temperature in the PVT panel was lower than the demand for the DHW tanks, the heat was transferred to the cold buffer storage tank.

The heat pump charged the DHW tank while extracting heat from the buffer storage tank when the temperature level of the DHW tank dropped below a set value. This was typically after a tapping of DHW. As the heat pump charged the domestic hot water tank, energy was extracted from the cold storage, which could then be recharged by the PVT panels.

The PVT panels were connected to the tanks via 20 m forward and 20 m return copper pipes with an outer/inner diameter of 22/20 mm. The pipes were insulated with Aeroflex with a thickness of 19 mm. The pipes between the heat pump to the storage tanks were each 4.5 m and diameter 22/20 mm.

The PVT solar heating system was tested under real weather conditions from August 2017 to April 2018 with some periods of fall out due to maintenances and renovations issues. Table 1 lists the main components of the PVT/heat pump system.

Component	**Description**
PVT collector	3.1 m^2 PVT panel (WISC) from Racell Technologies
DHW storage	160 litres with two 0.75 m^2spiral heat exchangers
Cold storage	200 litres with two inlets/outlets in the upper part of the tank and two in the bottom part of the tank
Heat pump	Vølund F1155-6.
Controller	Technische Alternative UVR 63
Solar loop pump	Grundfos Alpha2 25-80

Table 1. Components overview.

An UVR 63 from “Technische Alternative” controlled the solar collector loop of the system and the internal control in the heat pump was used to maintain the required temperature level in the top of the DHW tank.

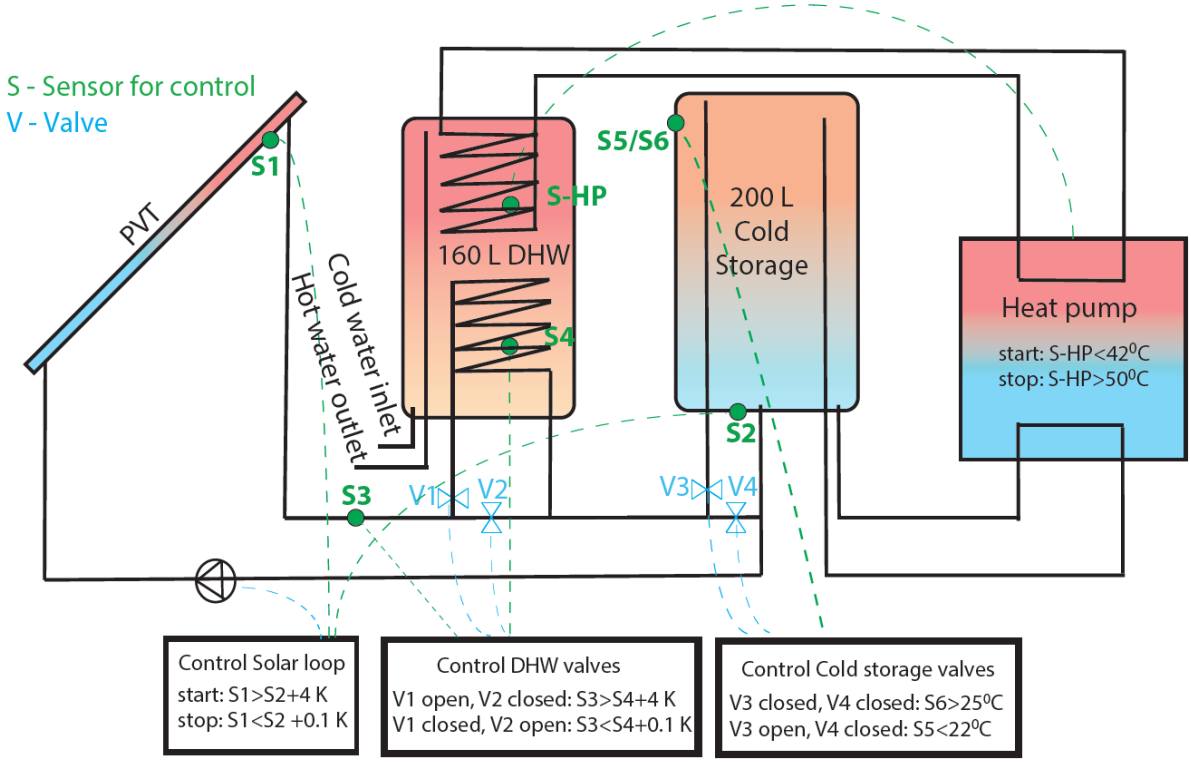

Figure 3. Illustration of the PVT system and the control strategy and sensor locations.

When the temperature on the back of the PVT panel near the outlet (S1) was 4 K higher than the bottom of the cold tank (S2) the flow in the collector loop started by switching on the solar collector loop pump. The pump remained on until the temperature of the PVT panel dropped below the temperature in the bottom of the cold tank. If the temperature in the pipe immediately before the DHW tank (S3) was 4 K higher than in the lower part of the DHW tank (S4), then the flow was directed through the lower heat exchanger spiral of the DHW tank by opening the valve V1 and closing the valve V2. When the temperature in the pipe before the DHW tank dropped to the same level as in the lower part of the DHW tank, then the flow bypassed the DHW tank by closing V1 and opening V2. As long as the temperature in the top of the buffer tank (S5/S6) was below 25°C, then the flow of the solar collector loop was directed through the buffer storage tank by having the valves V3 open and V4 closed. Otherwise, it was bypassed. This maximum temperature in the cold tank was due to the maximum allowed inlet temperature in the cold side of the heat pump of 30°C.

This control strategy allowed the collector loop to run even though heat was not transferred to any tank. This was when the buffer storage tank was fully heated to 25°C, the temperature in the PVT was higher than the buffer tank and the temperature in the bottom of the DHW tank was higher than in the PVT. A more advanced control strategy could have avoided this.

When the temperature in the top of the DHW tank (S-HP) dropped below 42°C, then the heat pump started and charged the top of the DHW tank to 50°C via the top spiral. When the heat pump discharged the cold tank and the temperature in the cold tank dropped below the ambient temperature, the PVT panels operated as energy absorbers and were used to extract heat from the ambient and recharge the buffer storage tank. This could be done even when no significant solar irradiance was available.

Detailed measurements were carried out with the aim to follow the detailed operation of the system. Temperatures in the pipes and in the stores and all important energy quantities of the system were measured. Some days of measurements were lost due to maintenance of the measurement and data logging equipment. Table 2 shows the days of complete measurements used for the performance analysis.

	Aug 2017	Sep 2017	Oct 2017	Nov 2017	Dec 2017	Jan 2018	Feb 2018	Mar 2018	Apr 2018
Days	25	30	31	30	31	27	27	31	12

Table 2. Days with complete measurements used for the performance analysis.

Concerning the PVT panel operation, energy absorber operation is assumed when the solar radiation level is below 50 W/m^2 and traditional solar thermal collector operation is assumed when the solar radiation level was higher than 50 W/m^2.

Two different solar fractions are used for evaluating the overall performance of the system. Solar fraction A only considers the tapped energy for the DHW draw off and the electricity consumed by the heat pump. Solar fraction B also includes the electricity produced in the PVT collector.

Solar fraction A is defined as: $SF_A = \frac{Q_{tap} - E_{system}}{Q_{tap}}$

Solar fraction B is defined as: $SF_B = \frac{Q_{tap} - E_{system} + E_{PV}}{Q_{tap}}$

where Q_{tap} is the energy tapped for the DHW draw offs, E_{sytem} is the energy consumed by the heat pump and solar collector loop pump and E_{PV} is the electricity produced in the PVT.

The net utilized solar energy was calculated as the energy tapped for DHW and the electricity produced in the PVT minus the electricity used by the heat pump and collector loop pump.

The net utilized solar energy is determined by $Q_{tap} + E_{PV} - E_{system}$

Figure 4 shows the measured average daily total solar irradiation on the PVT panel for each month over the test period.

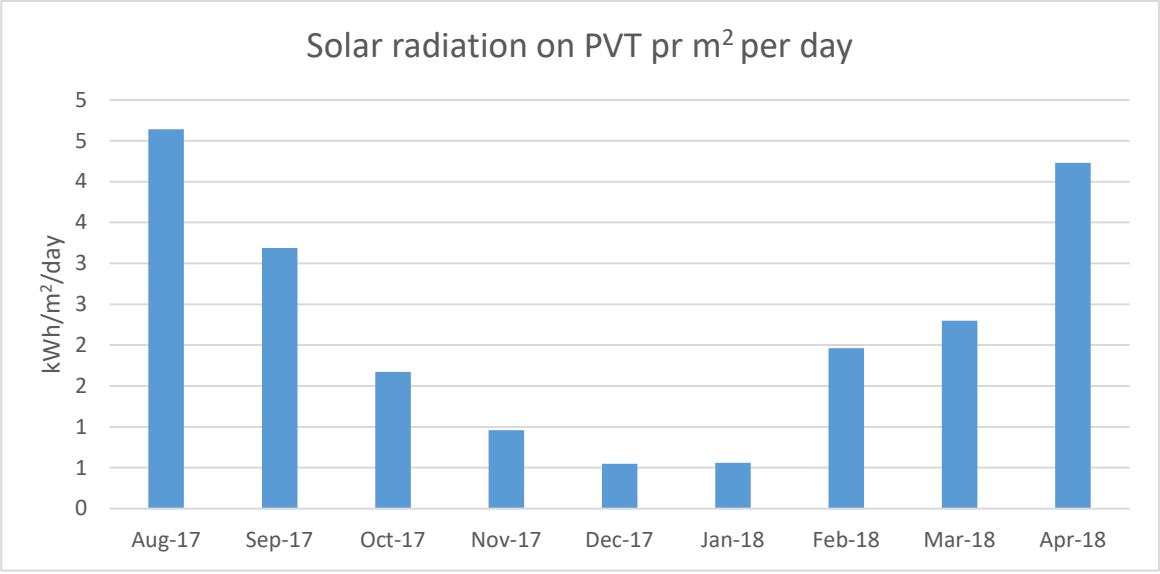

Figure 4. Measured daily average irradiation on the PVT panel for each month of the test period.

Figure 5 shows the PVT panel output. The PVT output is divided into electrical output from the PV, thermal output when the solar irradiance was higher than 50 W/m^2; and the energy absorber output when the solar irradiance was lower that 50 W/m^2. In addition, the average cold storage tank temperature, ambient air temperature and indoor temperature at the test facility are shown.

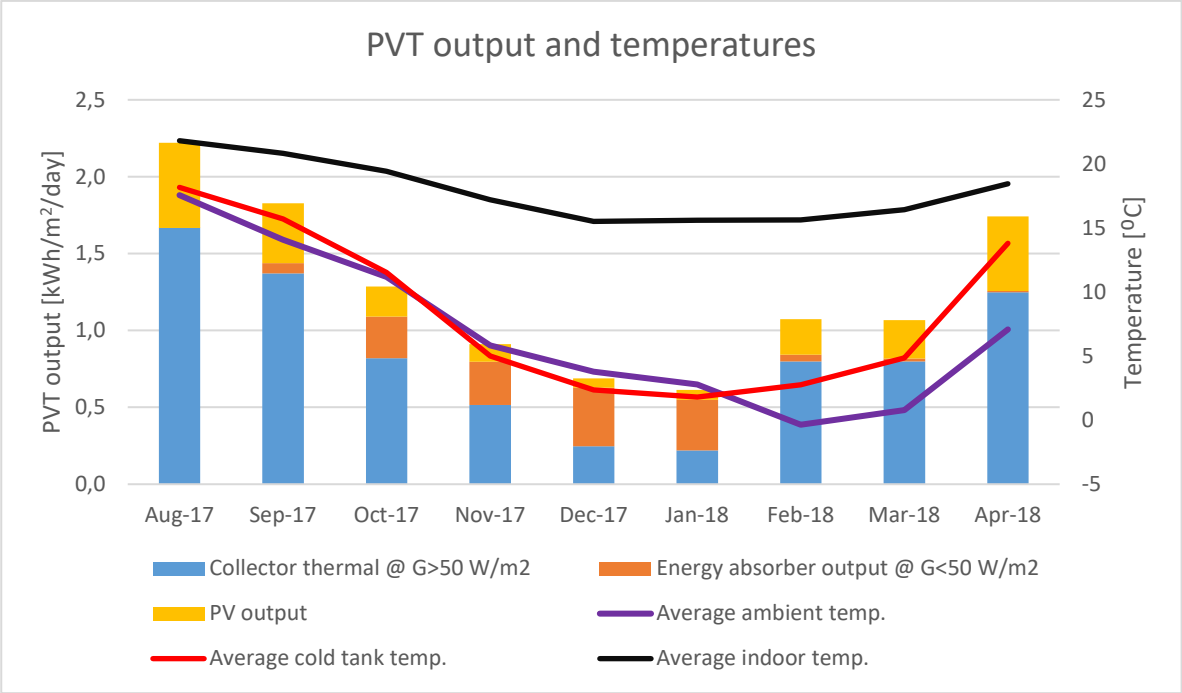

Figure 5. PVT panel thermal, energy absorber and PV output, monthly average ambient, indoor and cold storage tank temperatures.

From figures 4 and 5 can be seen that the PV output and the thermal output at irradiance levels higher than 50 W/m^2 are relatively proportional. For each months, the overall fraction of solar irradiation on the PVT panel converted into thermal output was in the range from 30 to 50 % as expected for an uninsulated collector.

December and January showed to have the highest levels of energy extracted from the ambient by the energy absorber. This was when the irradiance levels were very low and the temperature level in the cold storage tank was lower that the ambient temperature. In each month from October to January 0.8 to 1.1 kWh of heat was transferred from the PVT in energy absorber operation to the buffer storage tank per day. In this period, the ambient temperature was slightly higher than the cold storage tank and heat transfer was possible. The energy absorber function did add a considerable amount of energy to the system in these months.

In February and the following months only very little heat was transferred to the system from the PVT panel in energy absorber operation when the irradiance was lower that 50 W/m^2. This was due to the ambient temperature being lower than the temperature in the cold storage tank. In the months with solar irradiation higher than 2 kWh/m^2/day heat was primarily transferred to the storage tanks when the irradiance was higher than 50 W/m^2 and the thermal part of the PVT panel worked as a traditional solar collector.

Figure 6 shows the daily tapped energy quantities for the DHW draw offs, the energy extracted from the buffer storage, the energy delivered to the DHW tank by the heat pump and the electricity consumption of the heat pump. The figure indicates that there was a significant heat loss from the system. This was due to a relatively poor designed DHW tank with pipe connections in the top of the tank and a relatively long pipe connection between the tanks and the heat pump of 4.5 m. Also relatively short operation periods by the heat pump 20-40 minutes lead to significant extra pipe losses, as the heat pump started up, the pipes had to be heated first and the hot water energy left in the pipes between the heat pump and the tanks after the heat pump stopped was also lost.

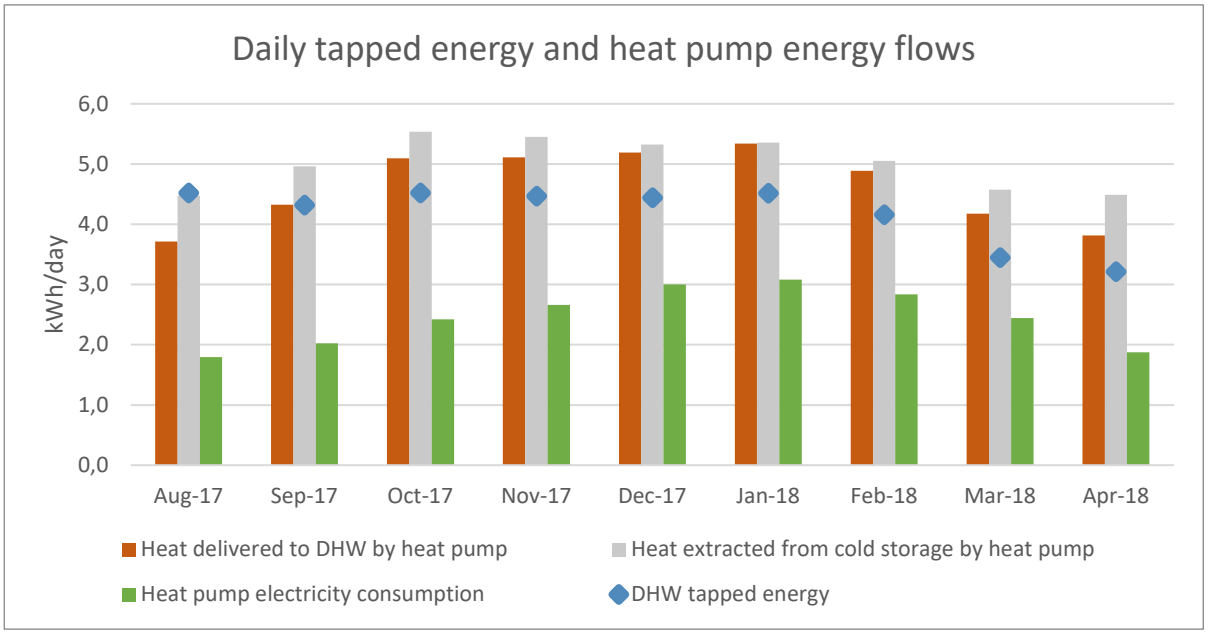

Figure 6. Daily tapped energy quantities and the energy extracted from the cold storage and delivered to the DHW tank and the electricity consumption by the heat pump. Normally the gray and green bar should add up to the brown bar.

Figure 7 shows the electricity consumption for the system (heat pump and collector loop pump), the produced electricity in the PV and the part of the produced electricity, which was directly used in the same minute as it was produced.

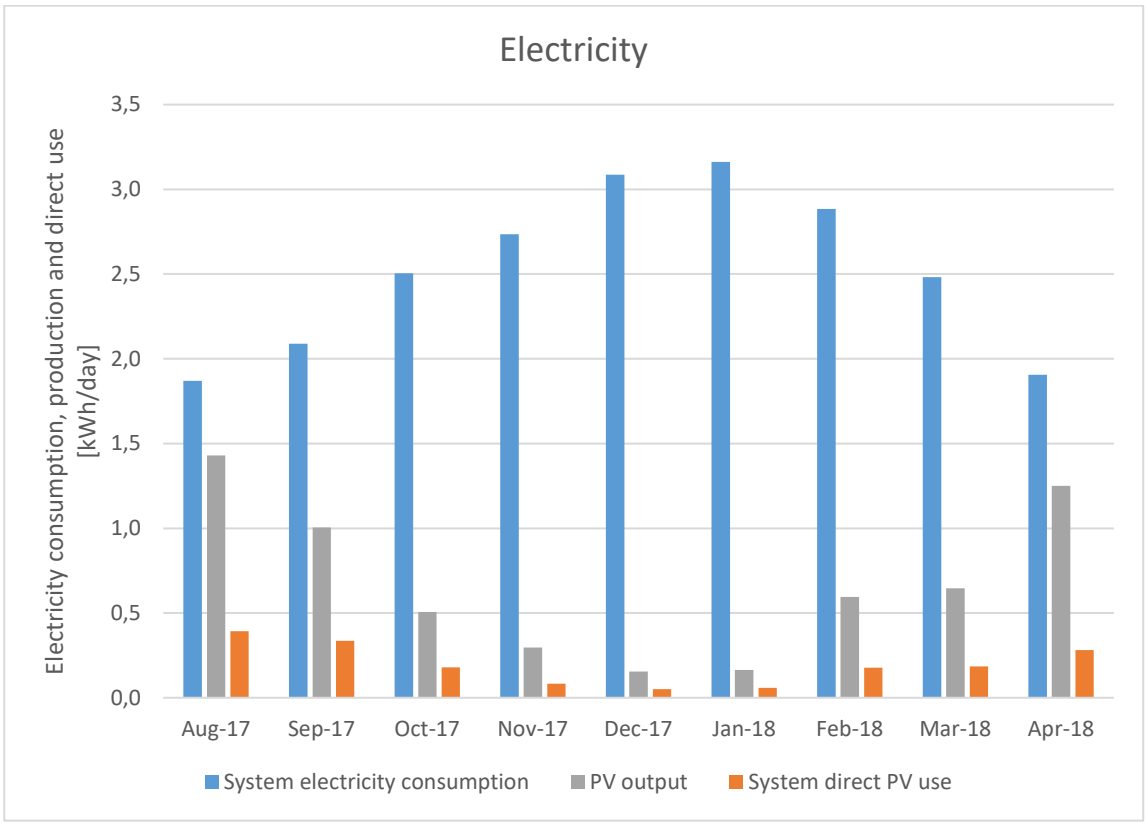

Figure 7. System electricity consumption, electricity produced in PVT and direct use.

It shows that for this size of a system, only a low fraction of the produced electricity in the PVT was consumed by the heat pump in the same period as it was generated. The main reason for this was that the heat pump operated with its own built in control independently of the solar irradiance level. A smart system control strategy may result in more direct electricity consumption if the demands were shifted to periods with high solar levels and the heat stored to periods of use. Further, for this sized specific system the power required by the heat pump was 800-1000 W in the summer period and 1200-1500 W in the winter period depending on the temperature level in the buffer storage tank. The installed PVT panel produced up to 330 W of AC electricity in sunny periods after the inverter losses. A larger PVT panel area or a smaller heat pump could lead to more direct electricity consumption.

Figure 8 shows the system solar fraction and the net utilized solar energy. It can be seen that in the sunny periods the solar fraction is up to 90 % with the potential of surpass 100 % in mid summer.

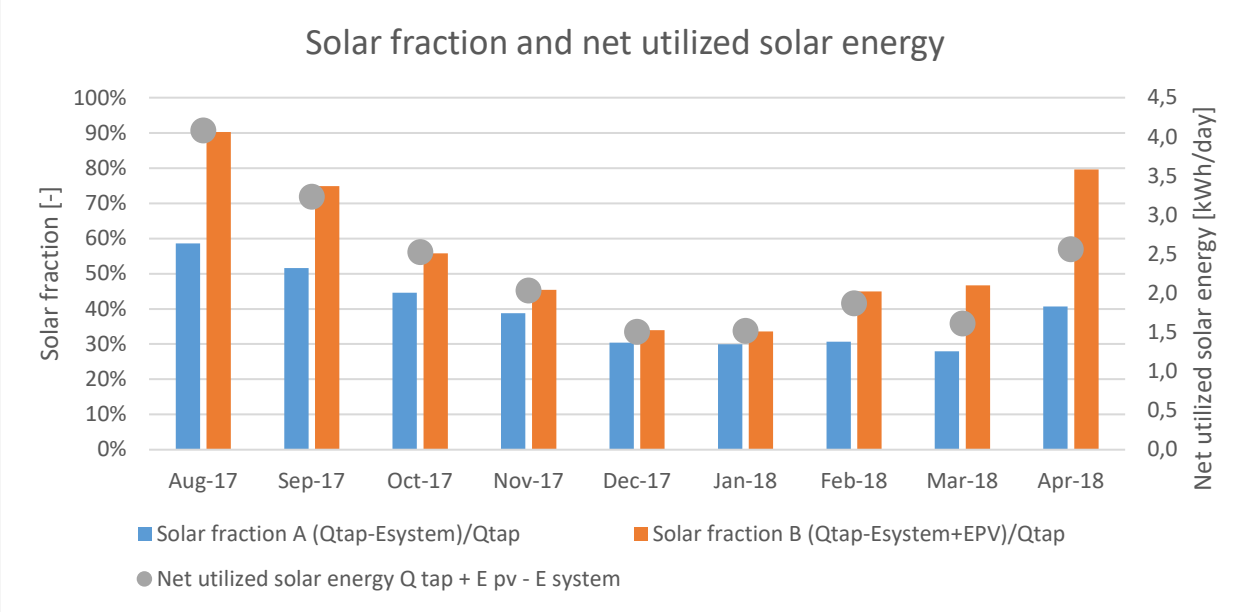

Figure 8. System solar fractions with and without electricity produced in the PVT and net utilized solar energy.

Table 3 shows the total accumulated values for the solar irradiation on the PVT panel, the thermal output at irradiance higher than 50 W/m^2, the energy absorber output, the tapped energy for the domestic hot water draw offs and the electricity consumption for the system.

Measurement period	Solar radiation on PVT collector	Collector output @ G>50 W/m^2	Energy absorber output @ G<50 W/m^2	DHW tapped energy	System electricity consumption
244 days	500 kWh/m^2	208 kWh/m^2	41 kWh/m^2	1034 kWh	628 kWh

Table 3. Overview of measurements of PVT system performance.

Table 4 shows the total accumulated values for the electricity consumption of the heat pump, both the total and for the periods where it was in operation and in standby. In addition, the heat delivered to the domestic hot water tank and the heat extracted from the cold storage is listed.

Heat pump electricity consumption	In operation electricity consumption	Standby electricity consumption	Heat delivered to DHW tank	Heat extracted from cold storage
612 kWh	536 kWh	75 kWh	1146 kWh	1238 kWh

Table 4. Heat pump electricity consumption, total, in operation and standby periods as well as heat delivered to DHW tank and extracted from the cold storage.

Table 5 shows the electricity produced in the PVT, electricity directly used by the heat pump and the solar collector loop pump, total electricity consumption for the solar collector loop pump and the electricity delivered to the grid and used from the grid.

Electricity produced in PVT (after inverter)	Heat pump direct PV consumption	Collector loop pump electricity consumption	Collector loop pump direct PV consumption	Electricity to grid	Electricity from grid
151 kWh	37 kWh	22 kWh	8 kWh	106 kWh	583 kWh

Table 5. Electricity produced in the PVT, electricity directly used by the heat pump and the solar collector loop pump, total electricity consumption for the solar collector loop pump and the electricity delivered to the grid and used from the grid.

The electrical efficiency of the PVT was throughout the test period measured after the inverter to be up to 13.5 % in sunny conditions.

The analysis showed that the principle of solar PVT assisted two-tank heat pump system with the energy absorber function worked. However, the control strategy was not optimal and an improved control strategy would result in a better performance of the system. In addition, the component sizes and designs as well as the pipe lengths and sizes in the lab system caused significant extra losses in the system, which reduced the performance of the system. The cold storage tank need to be large enough so that the temperature in it does not drop significantly below the ambient air temperature as the heat pump runs. Sizing of the cold storage tank similar to the volume passing through the cold side of the heat pump during one charge period is suggested. In addition, an inlet design in the cold storage tank that limits mixing and results in a steep thermocline moving upwards can be beneficial to keep the cold side inlet temperature to the heat pump and thereby the COP as high as possible. Further experimental and simulation investigations can show performances of similar systems with improved component sizes and control strategy.

The experimental system investigation showed that the uninsulated PVT panels worked as both solar thermal collectors in sunny conditions and as energy absorbers in conditions with solar irradiance below 50 W/m^2. During sunny days in summer the energy for the DHW draw offs were mainly covered by direct heat from the thermal absorber of the PVT panel. In October to January up to 0.4 kWh/m^2/day of heat was transferred to the cold buffer storage tank by the PVT panel operating as energy absorber, when the solar irradiance was below 50 W/m^2.

As the heat pump charged the DHW tank after a DHW draw off and discharged the cold tank the PVT panel was working as energy absorber and reheated the cold tank to ambient temperatures in conditions where irradiance levels were low. The cold buffer storage tank connected to the cold side of the heat pump worked well as the source for the liquid-liquid heat pump, however the design of the system could be improved to reduce thermal losses. The COP of the heat pump was affected by the temperature in the cold storage tank and a larger tank with better inlet designs for improved stratification could enhance the performance of the system. The lab system has proven the system type but by optimizing the component sizing and control higher energy savings and solar fractions can be achieved.

A TRNSYS simulation model for the tested PVT/heat pump system was developed and validated by means of the measurements, Dannemand et al. (2020).

The daily measured and simulated electrical and thermal output of the PVT collector is shown for a test period from the start of August 2017 to the end of December 2017 in Figure 9. The deviation between the measured and calculated energy quantities were less than 1% over the entire measurement period. On a monthly basis, the deviations were less than 5%, except for the electrical output in the winter period, where the output was very low and the relative deviation therefore was somewhat higher.

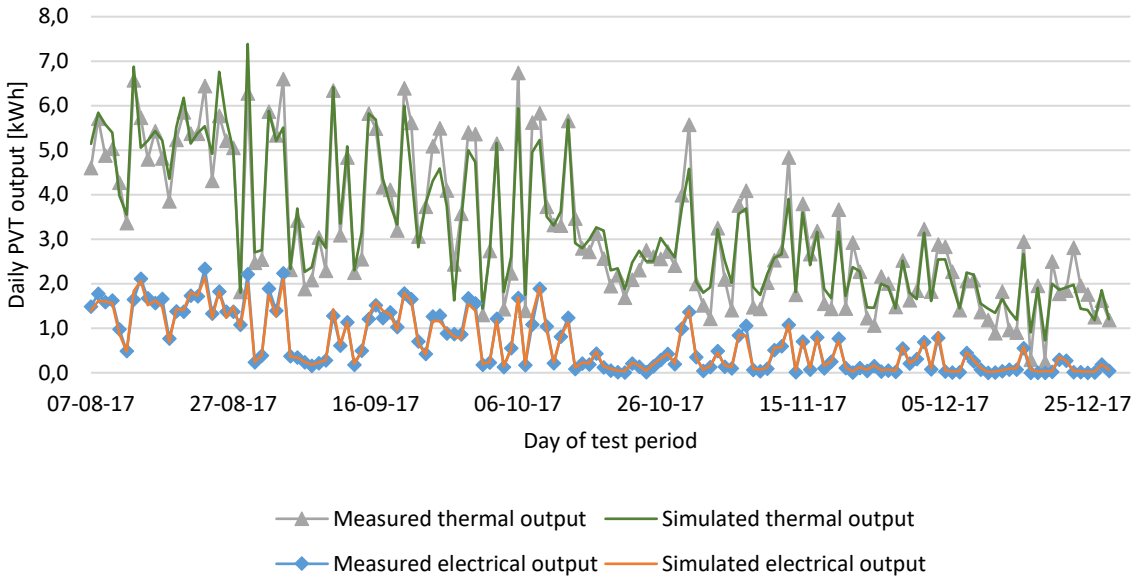

Figure 9. Daily measured and simulated electrical and thermal output of the PVT panel.

The measured and simulated electrical consumption and the thermal load output from the heat pump were compared over the test period in Figure 10. Over a monthly basis, the deviations between measurement and calculations were less than 4%.

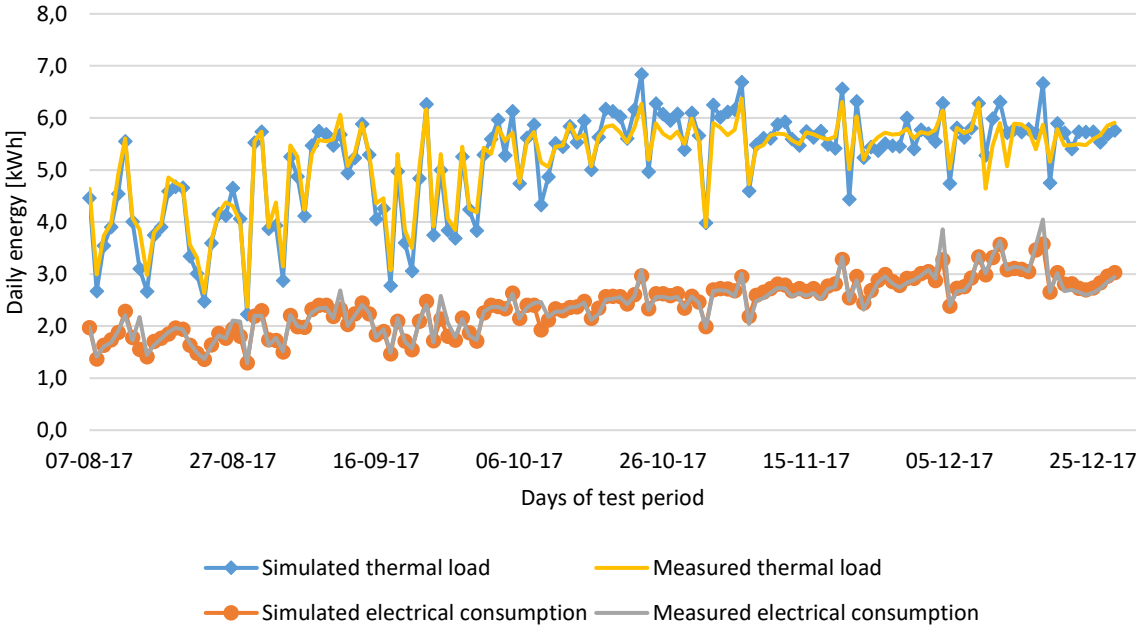

Figure 10. Measured and simulated daily electrical power consumption and thermal load delivered by pipe loop.

The measured and simulated energy transfer at key locations in the system were used to validate the full model against the measurements. Table 6 shows the measured and simulated energy quantities for tapped DHW, thermal and electrical output of the PVT panel, electrical consumption of the heat pump, heat delivered to the DHW tank by the heat pump and heat extracted from the buffer storage by the heat pump.

Month	Thermal collector output [kWh/day]		Tapped DHW [kWh/day]		PV electrical output [kWh/day]		Heat pump electrical consumption [kWh/day]		Heat delivered to DHW by heat pump [kWh/day]		Heat extracted from buffer storage by heat pump [kWh/day]	
	M	S	M	S	M	S	M	S	M	S	M	S
Aug.	5.16	5.16	4.3	4.52	1.52	1.53	1.74	1.84	4.04	3.96	4.4	4.64
Sept.	4	3.98	4.35	4.32	0.92	0.92	2.05	2.12	4.95	4.85	5.06	5.12
Oct.	3.29	3.27	4.33	4.52	0.57	0.55	2.38	2.31	5.19	5.47	5.49	5.26
Nov.	2.25	2.32	4.43	4.47	0.32	0.3	2.65	2.65	5.33	5.57	5.47	5.25
Dec.	1.74	1.81	4.52	4.51	0.22	0.19	3.14	2.97	5.46	5.65	5.39	5.14
Total	16.4	16.5	21.9	22.3	3.6	3.5	12.0	11.9	25.0	25.5	25.8	25.4

Table 6. Measured (M) and simulated (S) energy quantities in kWh/day for full model validation.

Table 7 illustrates the deviations between the previously mentioned quantities. It can be observed that the deviations between the measured and simulated values were less than 6% for each period and key location except for the electrical output of the PVT panel in December. Since the energy quantities calculated with the model is in good agreement with the measured energy quantities it is estimated that the model is validated and suitable for optimization of the system based on calculations with different system designs.

Month	Thermal collector output	Tapped DHW	PV electrical output	Heat pump electrical consumption	Heat delivered to DHW by heat pump	Heat extracted from buffer storage by heat pump
Aug.	0%	5%	1%	5%	-2%	5%
Sept.	-1%	-1%	0%	3%	-2%	1%
Oct.	-1%	4%	-3%	-3%	5%	-4%
Nov.	3%	1%	-6%	0%	5%	-4%
Dec.	4%	0%	-14%	-6%	3%	-5%
Total	1%	2%	-1%	-1%	2%	-2%

Table 7. Deviations between the simulated and the measured energy quantities for full model validation.

Figure 11 shows calculated yearly solar thermal fraction defined as the ratio between the heat produced by the PVT panel and the heat supplied to the heating system for different panel areas, buffer tank volumes and

domestic hot water volumes. Weather data from the Danish Test Reference Year are used for the calculations. The system covers a domestic hot water consumption of 100 L per day heated from 10°C to 50°C with hot water draw offs three times per day, at 7 am, at noon and at 7 pm. The tested (reference) system is presented by the orange bars in all figures and its level is also indicated by a dashed black line.

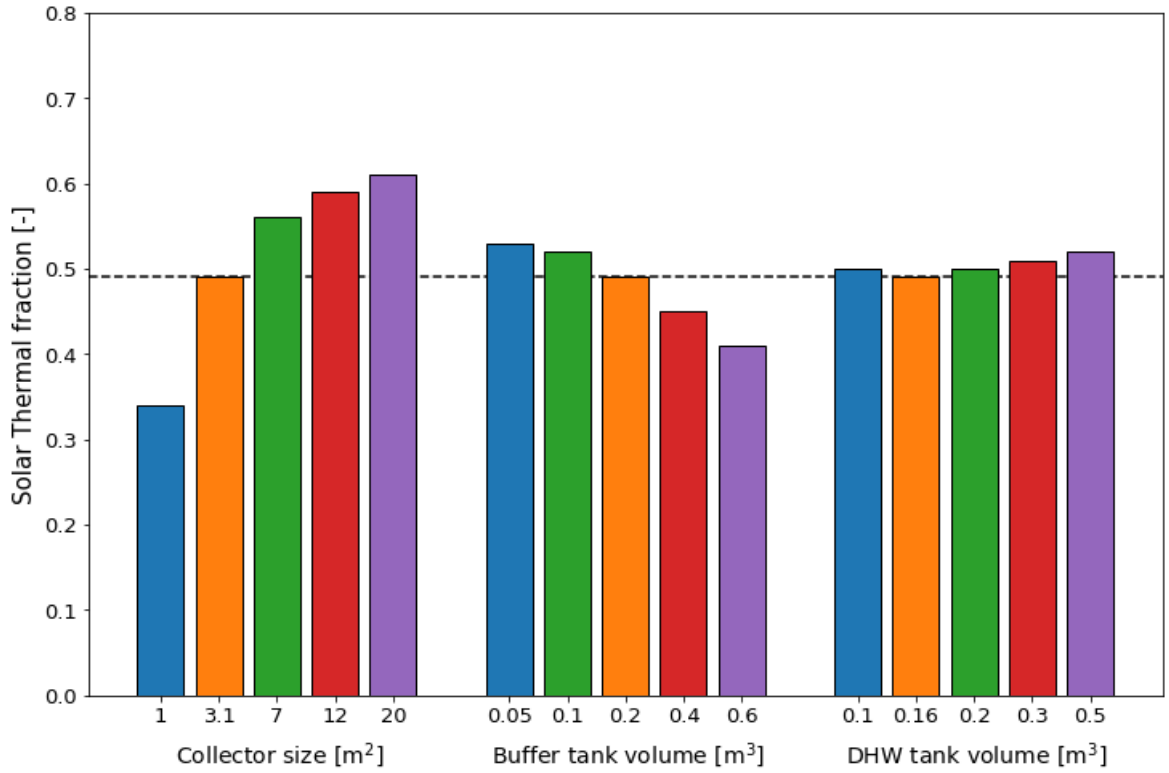

Figure 11. Solar thermal fraction for panel size, buffer and DHW tank volume parametric analysis.

The reference system's yearly solar thermal fraction was 0.49. By using a larger PVT panel area, the solar thermal fraction of the system can be improved. The thermal performance of the system can also be increased by decreasing the buffer tank volume, while the domestic hot water tank volume does not significantly influence the thermal performance of the system. The calculations shows that the system is somewhat oversized, since smaller tanks would increase its thermal performance.

Figure 12 shows the yearly solar electrical fraction defined as the ratio between the electrical energy produced by the PVT panel and the electrical energy used by the heating system for the system with different sizes.

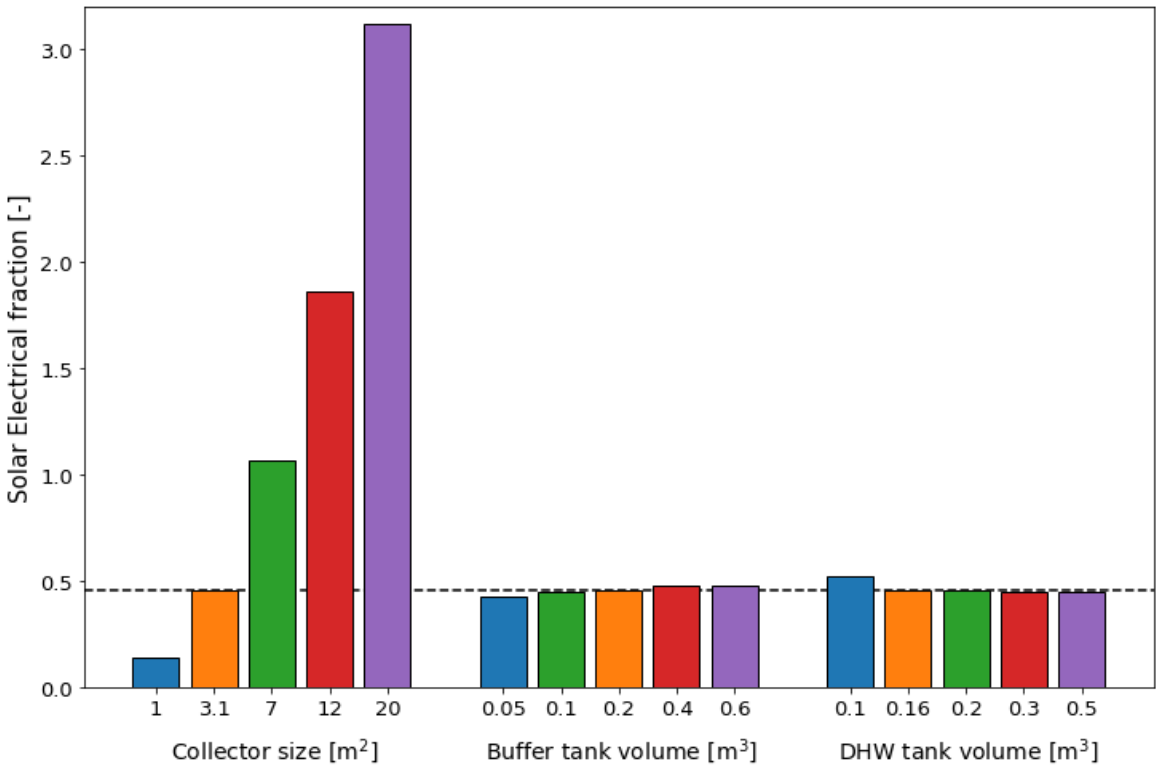

Figure 12. Solar electrical fraction for panel size, buffer and DHW tank volume parametric analysis.

The yearly solar electrical fraction of the reference system was 0.46. An increase in the PVT panel area can cause a very steep increase in the solar electrical fraction, due to larger electrical production. The volumes of the buffer tank and the domestic hot water tank are not strongly influencing the electrical performance of the system.

From figure 11 and 12, it can be observed that a larger panel area is always beneficial regarding electricity production while there is a limit in how much thermal energy from the PVT panel can be utilized by the system. This suggests that, from a certain panel area and on, it might be more beneficial to install PV panels instead of increasing the PVT panel area.

The investigations of a new heating system consisting of a heat pump, PVT panels, a buffer and a domestic hot water tank for supplying domestic hot water showed that:

- The system design is suitable for single family houses in Denmark.
- A larger PVT panel area is always beneficial regarding electrical production, but there is a limit regarding how much thermal energy can be utilized. Therefore, from a certain panel area and on, it is more beneficial to install PV panels instead of increasing the PVTpanel area.
- For a system that produces only domestic hot water, the thermal performance of the system increased when the size of the buffer and the DHW tank were the smallest investigated. This indicated that the system under investigation was somewhat oversized.
- For a system providing both space heating and domestic hot water supply the system must be optimized with regard all components: PVT panel area, heat pump size, buffer tank volume and domestic hot water tank volume. The developed simulation model is valuable in connection with this optimization.

5.2 Cooling by means of PVT panels

There are two cooling effects in connection to a PVT panel. **By lowering the Photovoltaic cell operating temperature**, more solar energy can be harvested as electricity. The gain is roughly 0.4% per K lower cell temperature for a silicon solar cell. For operation in a system with a heat pump and/or ground thermal storage, the cell operating temperature can be lowered significantly compared to a PV panel without cooling, maybe 25 K lower, corresponding to an electrical energy output increase by 10%. This percent value is relative, so for a PV module with 20% efficiency it corresponds to a 2% absolute efficiency improvement. Not a dramatic effect. But still very valuable if created cheaply. An example of the magnitude of this effect can be seen in figure 13 in a ScenoCalc simulation for Copenhagen and for an unglazed Racell PVT module.

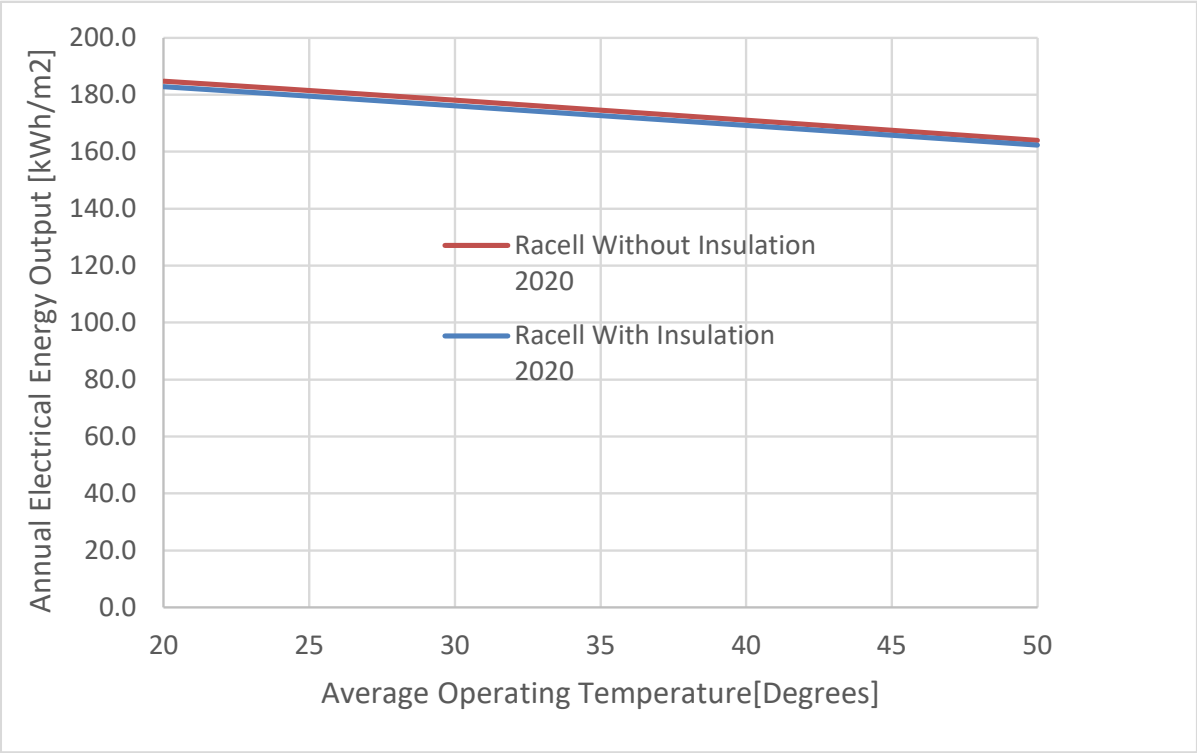

Figure 13. Increase of the annual electrical performance due to lowering the cell temperature. Climate Copenhangen for a Racell unglazed PVT module.

The PVT panel can also be used to cool a house or office, often via a cold storage tank by circulation of fluid through the PVT at no, or low solar radiation conditions. Preferably at night. The PVT thermal performance gain model is approximately valid also for cooling at no sun, even if there are small second order effects when the total heat flow goes the other way out from the collector fluid at night, instead of into the fluid daytime. The solar radiation part of the PVT model is still used, but goes of course to a low, or zero value at night. (The visible spectrum radiation, from the moon or stars is completely negligible for this energy balance. Our eyes are just extremely sensitive to low light levels.) But the heat loss parts of the model is still active and losses occur by mainly thermal radiation to the clear sky, clouds and surroundings, plus natural and forced convection to the air by wind and boyancy forces. Conduction losses are very small and can be neglected.

A calculation for Copenhangen Taastrup data shows that the cooling potential to low temperatures is quite limited in summer months when the need is expected.

There is some undertemperature possible due to radiative cooling to clear sky, but this requires very low wind speed, at the same time with clear sky (no clouds), to utilize this potential. Figure 14 shows the results

based on the test parameters derived for the Racell PVT module summer 2020. From 20°C operating temperature and up there is a clear cooling effect all summer. Only hours with low solar radiation when there is a potential, are summed up each month.

This limited cooling potential, can still be worth to consider as it is almost free, if the system can be switched between different operating modes day and night.

Lower operating temperatures than 10°C are not shown, as then condensation of moisture from the air will occur onto the PVT surface and limit further cooling. This level of modelling could be investigated further. Simulation models are availbale for that when a PVT is working against a Heat Pump. But then it is not free cooling.

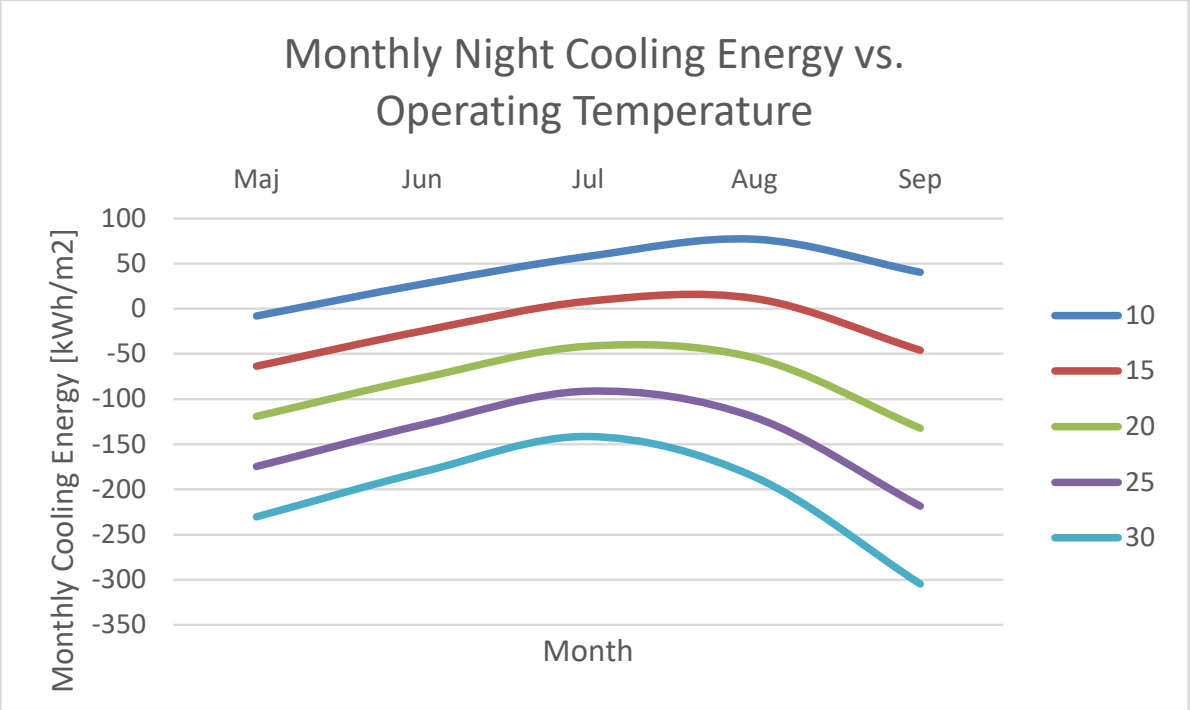

Figure 14. Cooling energy (negative on the y-axis) for the Copenhagen Climate, based on the test parameters derived for the Racell PVT module summer 2020. From 20°C operating temperature and up there is a cooling potential.

5.3 Efficiency of PVT panels

A Racell PVT panel with and without back side insulation has been long term tested outdoors at the test facilities of DTU Civil Engineering under real weather conditions. The PV part has been active all the time and both thermal and electrical output has been measured accurately with high time resolution. Figure 15 shows the PVT panel and measuring equipment.

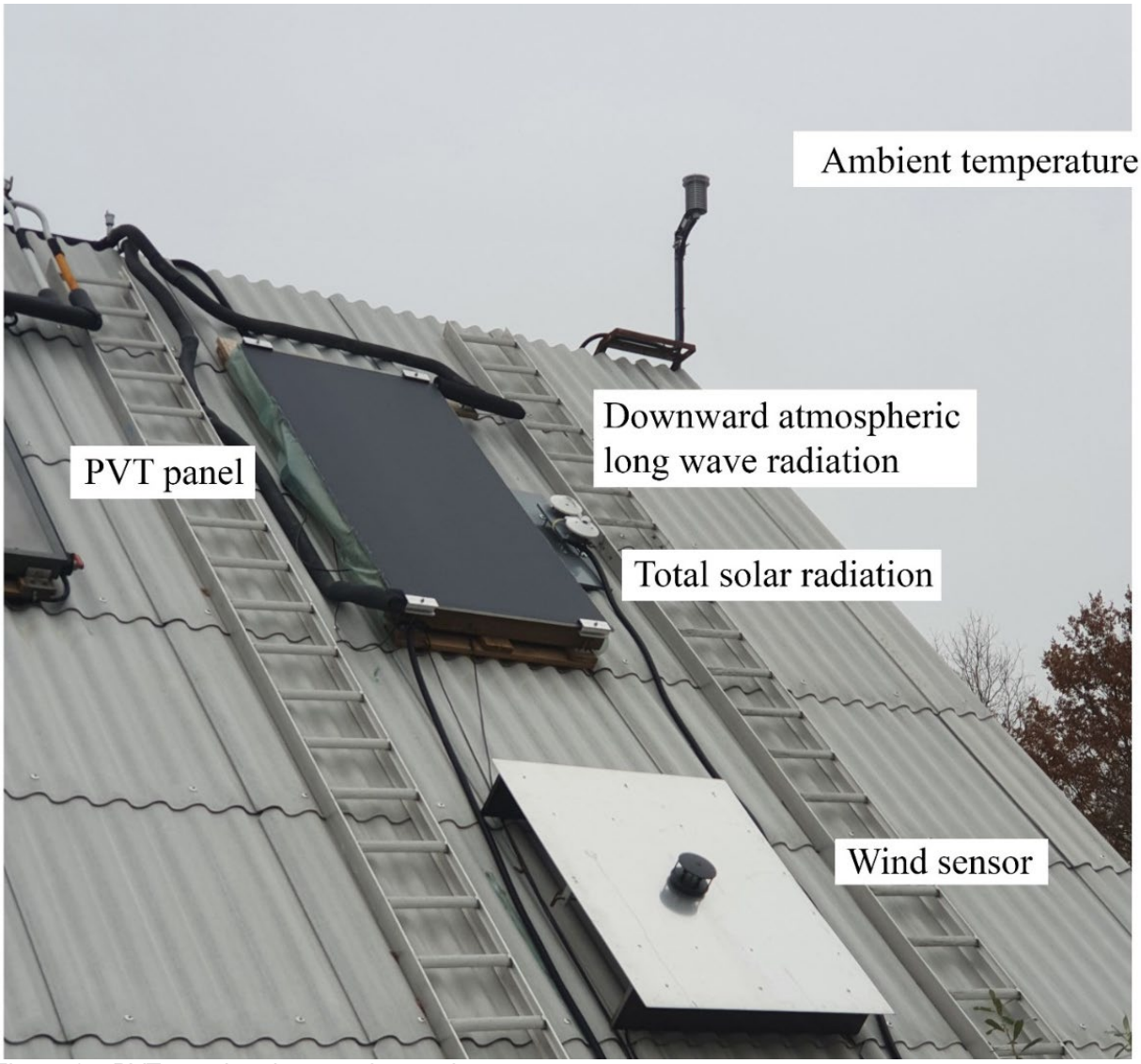

Figure 15. PVT panel and measuring equipment.

The PVT panel's gross area was 1.99 m x 0.96 m = 1.91 m^2. In the variant with back side insulation the insulation thickness was 100 mm of stone wool insulation at the back of the PVT panel.

The test rig has been carefully designed and the test has been run according to the specifications in the ISO 9806 world standard.

The panel tilt was 45° and the panel was facing due south.

The short term measured data has been collected and averaged and selected for analysis according to the standard.

The electrical performance has also been modelled and checked during the test but no parameter analysis is done, as this is not part of the standard. The PV parameters used were Standard Test Efficiency at STC of 18% (1000 W/m^2 and 25°C cell temperature) and a PV cell temperature dependence of 0.4% per K and an incidence angle dependence with b_0=0.1. This was shown to fit closely to measured data. These PV parameters were also used in ScenoCalc PVT annual kWh simulations.

The thermal parameter results are shown in table 8 for the two variants of the panel.

The thermal performance of the PVT panel is determined by the equations

$$\dot{Q} = A\left[\eta_{0,b}\,K_b(\boldsymbol{\theta})G_b + \eta_{0,b}\,K_d\,G_d - a_1\,(T_{mean} - T_{amb}) - a_2\,(T_{mean} - T_{amb})^2 - a_3\,u'(T_{mean} - T_{amb}) + a_4\,(E_L - \sigma\,T_{amb}^4) - a_5\frac{dT_{mean}}{dt} - a_6\,u'\,G_{hem}\right]$$

$$\mathbf{K_b(\theta)} = 1 - \mathbf{b_0} \bullet [(1/\cos\theta)\text{-}1]$$

where:
$\dot{Q}$ is thermal power of PVT panel, W
A is gross area of PVT panel, m²
$K_b(\theta)$ is the incidence angle modifier for the beam radiation, -
θ is incidence angle for beam radiation, °
$\eta_{0,b}$ is peak panel efficiency, -
K_d is the incidence angle modifier for the diffuse radiation, -
G_b is the beam radiation on the panel, W/m²
G_d is the diffuse radiation on the panel, W/m²
G_{hem} is the total irradiance in the panel plane, W/m²
a1 is heat loss coefficient of the panel at ambient temperature, W/(m²K)
a2 is temperature dependence of heat loss coefficient of the panel, W/(m²K²)
T_m is the mean solar collector fluid temperature, °C
T_{amb} is the ambient air temperature, °C
a_3 is wind speed dependence of the heat loss coefficient, J/(m³ K)
a_4 is the sky temperature dependent heat loss coefficient, -
a_5 is effective thermal capacity, J/(m² K)
a_6 is wind speed dependence of the zero loss efficiency, s/m
E_L is the longwave irrradiance, W/m²
u' is the reduced air speed, m/s
σ is the Stefan-Boltzmann constant, W/m²K⁴
t is time, s
b_0 is an incidence angle dependency constant, -

Figure 16 shows the incidence angle dependence of beam zero loss efficiency and the incidence angle modifier. The incidence angle modifier determined by the b0 equation that was used in the annual kWh calculations is also shown. Only statistically significant parameters with a t-ratio above 3 according to the ISO 9806 standard, are shown in table 8 and then used in the annual ScenoCalc kWh calculations.

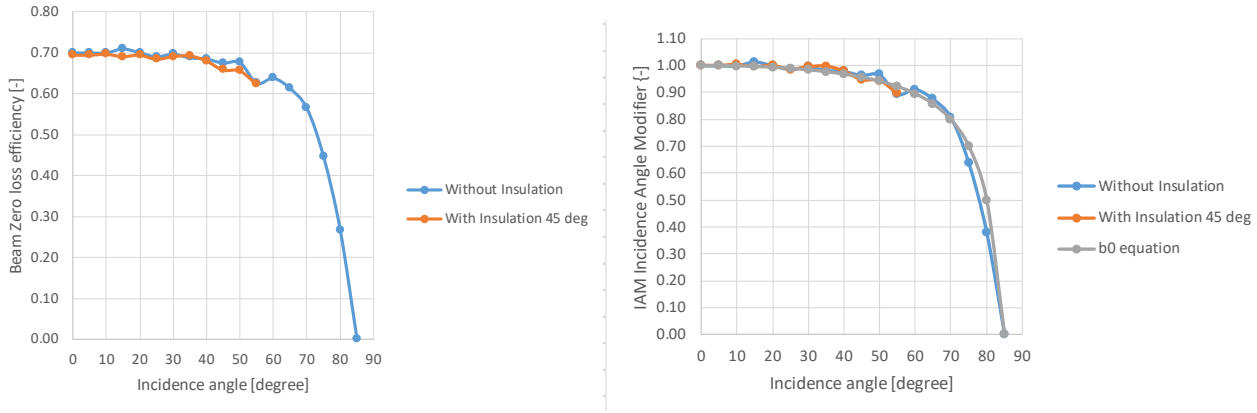

Figure 16. Incidence angle dependency.

Racell PVT Test 2020 Without Insulation					Racell PVT Test 2020 With Insulation 45 deg					
Parameter	Value				Parameter	Value				
n0_diffuse	0.6757				n0_diffuse	0.6564				
a1	14.1291				a1	10.8803				
a2	0				a2	0				
a3	6.6023				a3	2.3717				
a4	0				a4	0.4138				
a5	54800				a5	54460				b0 equation
a6	0.0486				a6	0.0445				0.105
Kdiff	0.965286				Kdiff	0.945821				
Incidangle	n0_beam		IAM		Incidangle	n0_beam		IAM		
0	0.7000		1.0000		0	0.6940		1.0000		1.0000
5	0.7000		1.0000		5	0.6940		1.0000		0.9996
10	0.7000		1.0000		10	0.6961		1.0030		0.9984
15	0.7098		1.0140		15	0.6905		0.9950		0.9963
20	0.7005		1.0007		20	0.6941		1.0001		0.9933
25	0.6905		0.9864		25	0.6842		0.9859		0.9891
30	0.6968		0.9954		30	0.6906		0.9951		0.9838
35	0.6882		0.9831		35	0.6924		0.9977		0.9768
40	0.6850		0.9786		40	0.6800		0.9798		0.9679
45	0.6752		0.9646		45	0.6578		0.9478		0.9565
50	0.6764		0.9663		50	0.6559		0.9451		0.9417
55	0.6261		0.8944		55	0.6236		0.8986		0.9219
60	0.6382		0.9117		60	0.4641		0.6687		0.8950
65	0.6128		0.8754		65			0.0000		0.8566
70	0.5648		0.8069		70			0.0000		0.7980
75	0.4461		0.6373		75			0.0000		0.6994
80	0.2657		0.3796		80			0.0000		0.5005
85	0.0000		0.0000		85			0.0000		0.0000
90	0.0000		0.0000		90			0.0000		0.0000

Table 8. Solar collector efficiency of two PVT panels.

Based on the determined efficiency expressions calculations were carried out to determine the monthly and the yearly performances of the PVT panels. The yearly thermal output is shown in figure 17 for the Copenhagen climate.

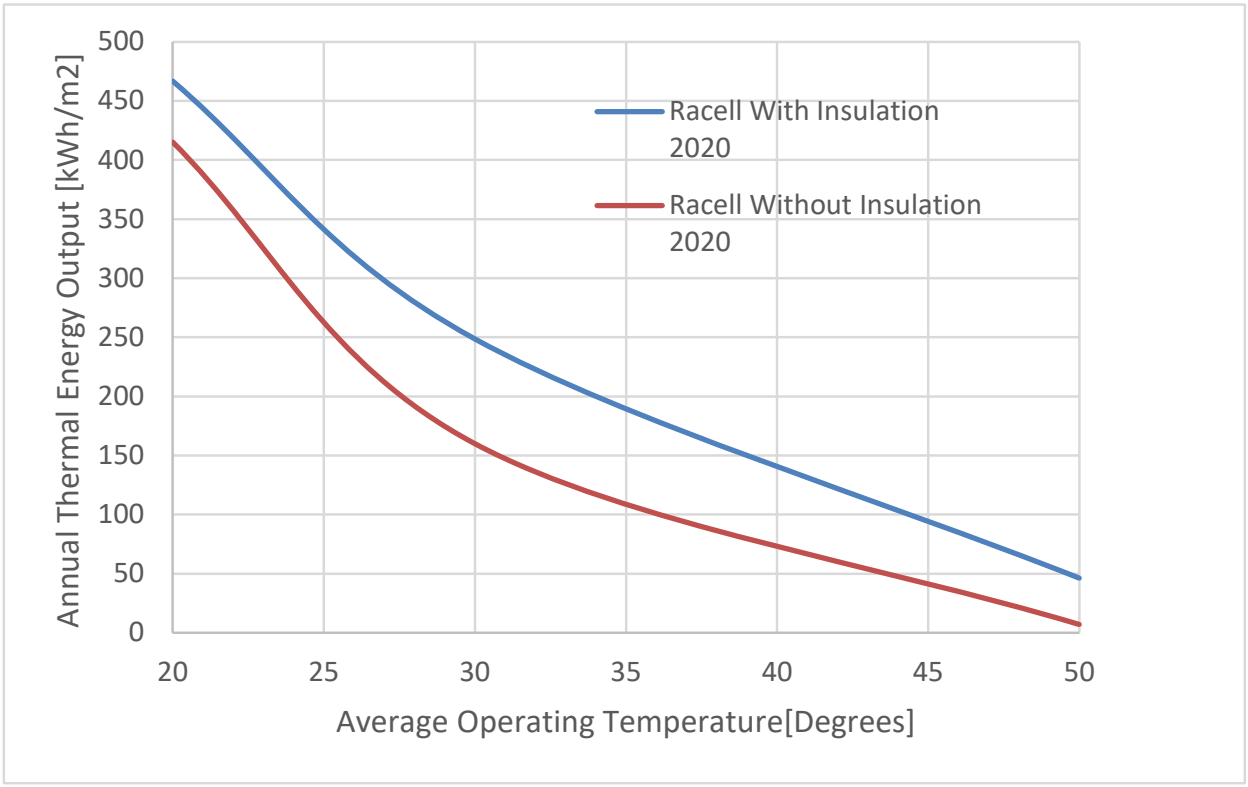

Figure 17. Yearly thermal performance of two PVT panels as function of mean collector fluid trremperature.

The yearly electrical output per m² is shown in figure 18.

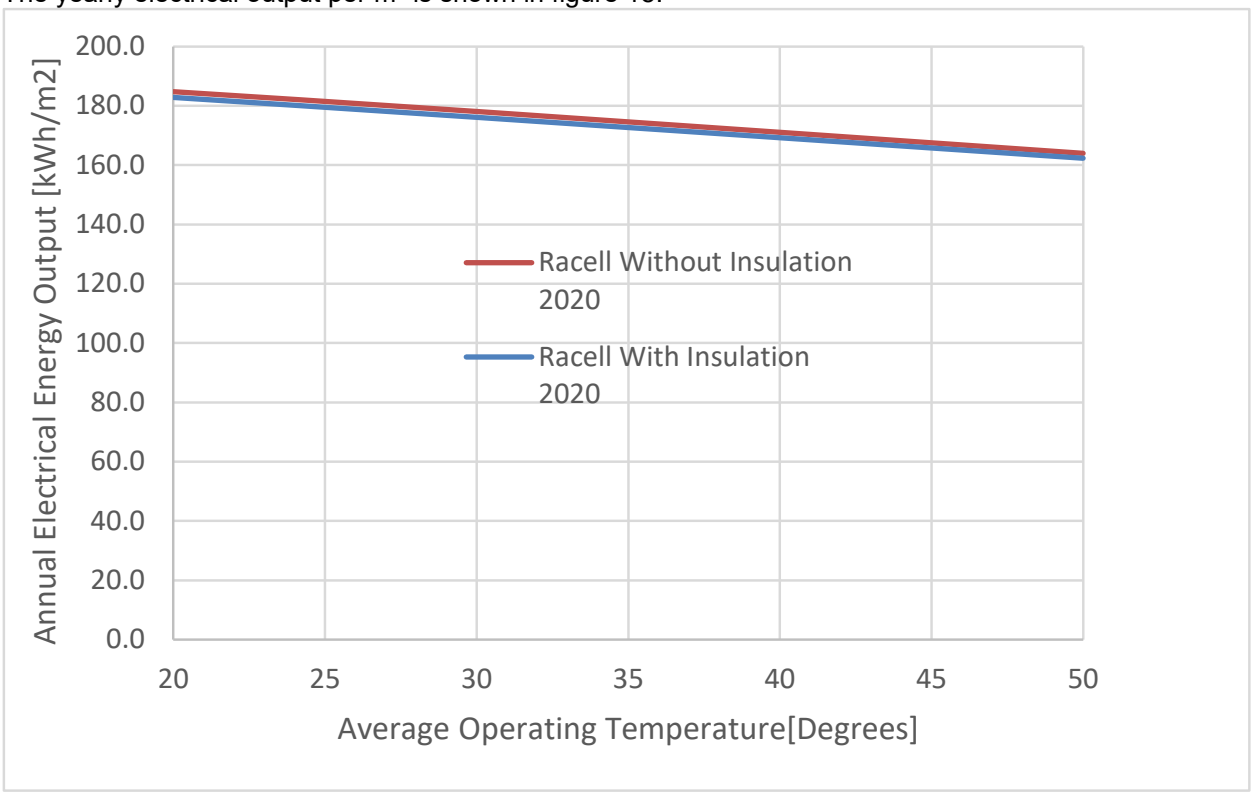

Figure 18. Yearly electricity production of two PVT panels as function of the mean collector fluid temperature.

Monthly calculated performances of the Racell PVT panel without insulation and with back side insulation are shown in figure 19 and 20. The calculations are carried out with the Scenocalc tool for PVT collectors, version 3.10d.

Results from the Solar Energy Output Calculator (SEnOCalc)
Version 3.10 (PRELIMINARY, January 2012)

Identification label for the solar collector: Not specified
Date of evaluation: 3 November, 2020
Evaluation method: Quasi Dynamic Testing

Thermal yield per collector module (kWh/module)

	Total irradiance	Yield for three collector mean temperatures		
		20°C	30°C	50°C
January	23	0	0	0
February	52	3	0	0
March	98	9	1	0
April	140	36	12	0
May	159	54	21	0
June	150	70	29	1
July	152	91	39	3
August	129	75	30	2
September	133	54	21	0
October	79	17	4	0
November	39	5	0	0
December	16	1	1	0
Year	**1,171**	**415**	**160**	**7**

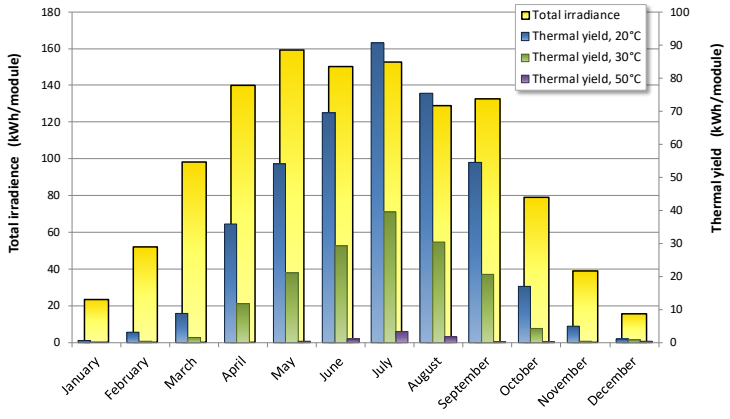

PV output per collector module (kWh/module)

	Total irradiance	Yield for three collector mean temperatures		
		20°C	30°C	50°C
January	23	3.7	3.6	3.3
February	52	8.3	7.9	7.3
March	98	15.7	15.1	13.9
April	140	22.1	21.3	19.6
May	159	25.0	24.1	22.2
June	150	23.5	22.7	20.9
July	152	23.9	23.1	21.3
August	129	20.3	19.6	18.1
September	133	20.9	20.2	18.6
October	79	12.6	12.1	11.1
November	39	6.2	5.9	5.5
December	16	2.5	2.4	2.2
Year	**1,171**	**184.7**	**178.0**	**164.0**

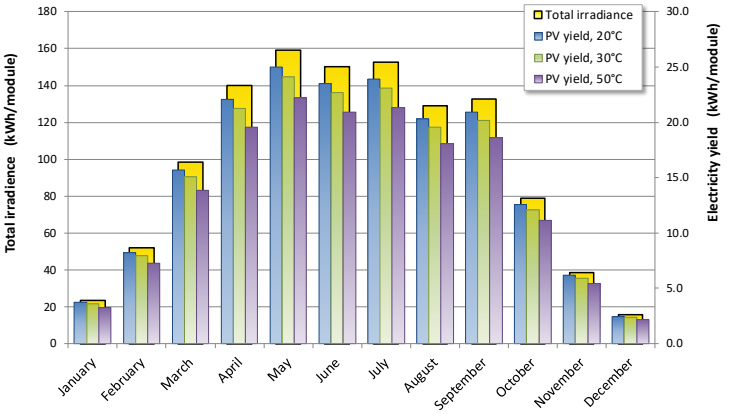

Location: Copenhagen
Longitude: -12.30 *(positive longitude = west of the prime meridian)*
Latitude: 55.67
Time period for climate data: 2012-RefDTU

Collector parameters (based on the aperture area)

Aperture area	1 m²	
$F'(\tau\alpha)_{en}$	0.7	
$K_{\theta,d}$	1.0	$(\Rightarrow \eta_0 = F'(\tau\alpha)_{en} \cdot (K_{\theta,b}(15°) \cdot 0.85 + K_{\theta,d} \cdot 0.15) = 0.694)$
c_1	14.1 W/m² K	$\Rightarrow a_1 = c_1 + 3 \cdot c_3 = 33{,}9351$ W/m²K (including wind 3 m/s)
c_2	0 W/m² K²	$\Rightarrow a_2 = c_2 = 0$ W/m²K²
c_3	6.602 J/m³ K	
c_4	0	
c_6	0.0486 s/m	
Wind correction	0.5	

PV parameters (based on the aperture area)

Absorber area	1 m²	
$P_{max\ PV}$	180 W	
$PV_{temp\ dep}$	0.004 1/°C	
C_{bond}	150 W/m²/K	
PR_{sys}	0.9	*(System performance ratio)*

Type of tracking: No tracking
Tilt angle: 45°
Azimuth angle: 0°

IAM Type: Simple, one-direction

Figure 19. Monthly performances of the PVT panel without back side insulation.

Results from the Solar Energy Output Calculator (SEnOCalc)
Version 3.10 (PRELIMINARY, January 2012)

Identification label for the solar collector: Not specified
Date of evaluation: 3 November, 2020
Evaluation method: Quasi Dynamic Testing

Thermal yield per collector module (kWh/module)

	Total irradiance	Yield for three collector mean temperatures		
		20°C	30°C	50°C
January	23	2	0	0
February	52	7	3	0
March	98	19	8	0
April	140	46	25	4
May	159	62	35	6
June	150	73	41	8
July	152	89	50	12
August	129	74	40	8
September	133	61	32	6
October	79	24	11	1
November	39	9	3	0
December	16	1	1	1
Year	**1,171**	**467**	**248**	**46**

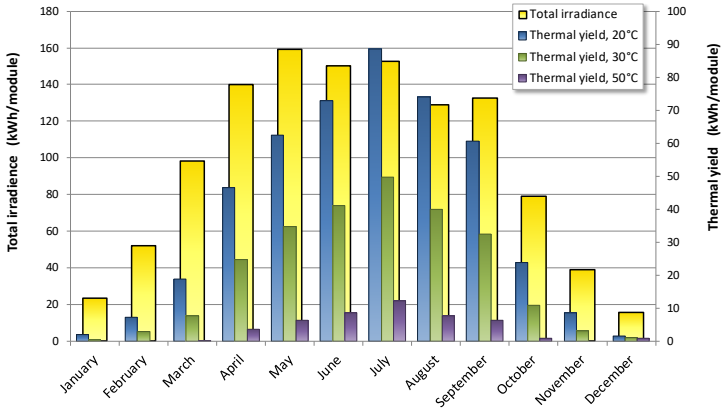

PV output per collector module (kWh/module)

	Total irradiance	Yield for three collector mean temperatures		
		20°C	30°C	50°C
January	23	3.7	3.6	3.3
February	52	8.2	7.9	7.2
March	98	15.5	14.9	13.7
April	140	21.9	21.1	19.4
May	159	24.8	23.9	22.0
June	150	23.3	22.4	20.7
July	152	23.7	22.8	21.1
August	129	20.1	19.4	17.9
September	133	20.8	20.0	18.4
October	79	12.5	12.0	11.0
November	39	6.1	5.9	5.4
December	16	2.4	2.4	2.2
Year	**1,171**	**182.9**	**176.2**	**162.3**

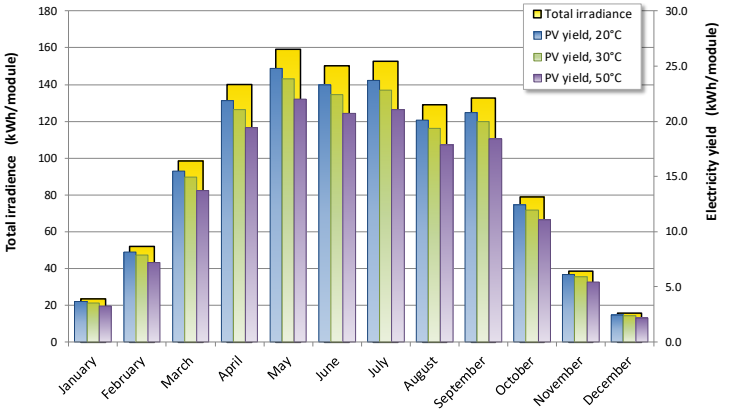

Location: Copenhagen
Longitude: -12.30 *(positive longitude = west of the prime meridian)*
Latitude: 55.67
Time period for climate data: 2012-RefDTU

Collector parameters (based on the aperture area)

Aperture area	1 m²	
$F'(\tau\alpha)_{en}$	0.694	
$K_{\theta,d}$	0.9	$(\Rightarrow \eta_0 = F'(\tau\alpha)_{en} \cdot (K_{\theta,b}(15°) \cdot 0.85 + K_{\theta,d} \cdot 0.15) = 0.686)$
c_1	10.9 W/m² K	$\Rightarrow a_1 = c_1 + 3 \cdot c_3 = 17{,}9954$ W/m²K (including wind 3 m/s)
c_2	0 W/m² K²	$\Rightarrow a_2 = c_2 = 0$ W/m²K²
c_3	2.3717 J/m³ K	
c_4	0.4138	
c_6	0.0445 s/m	
Wind correction	0.5	

PV parameters (based on the aperture area)

Absorber area	1 m²	
$P_{max\ PV}$	180 W	
$PV_{temp\ dep}$	0.004 1/°C	
C_{bond}	150 W/m²/K	
PR_{sys}	0.9	*(System performance ratio)*

Type of tracking: No tracking
Tilt angle: 45°
Azimuth angle: 0°

IAM Type: Simple, one-direction

Figure 20. Monthly performances of the PVT panel with back side insulation.

The investigations elucidated the efficiencies and the performances of the PVT panels. The efficiency expressions are useful in connection with planning, design and optimization of future PVT systems.

5.4 PVT panel integrated in concrete façade. Characterization and simulation model.

Two identical 2 m² PVT panels with monocrystalline solar cells produced by Racell Technologies were mounted on a free standing concrete wall, Dannemand et al. (2019). One panel was mounted directly in contact with the wall. The other panel was installed with 10 mm Styrofoam between the PVT panel and the concrete wall. The PVT panels were mounted vertically and were oriented facing south-west, as shown in figure 21. Measurements were taken from June to August 2019, at the test facility of the Department of Civil Engineering,

Technical University of Denmark.

Figure 21. PVT panels integrated into a concrete facade.

The pipes to and from the PVT panel were connected to a test rig where the forward temperature was controlled with a heating and cooling system. The equipment setup for maintaining a constant forward temperature to the panel is illustrated in figure 22. The panels were tested with four different operating temperatures: 15, 20, 25 and 30°C. The flow rate was kept constant through all the measurement period at 0.045 L/s for each panel.

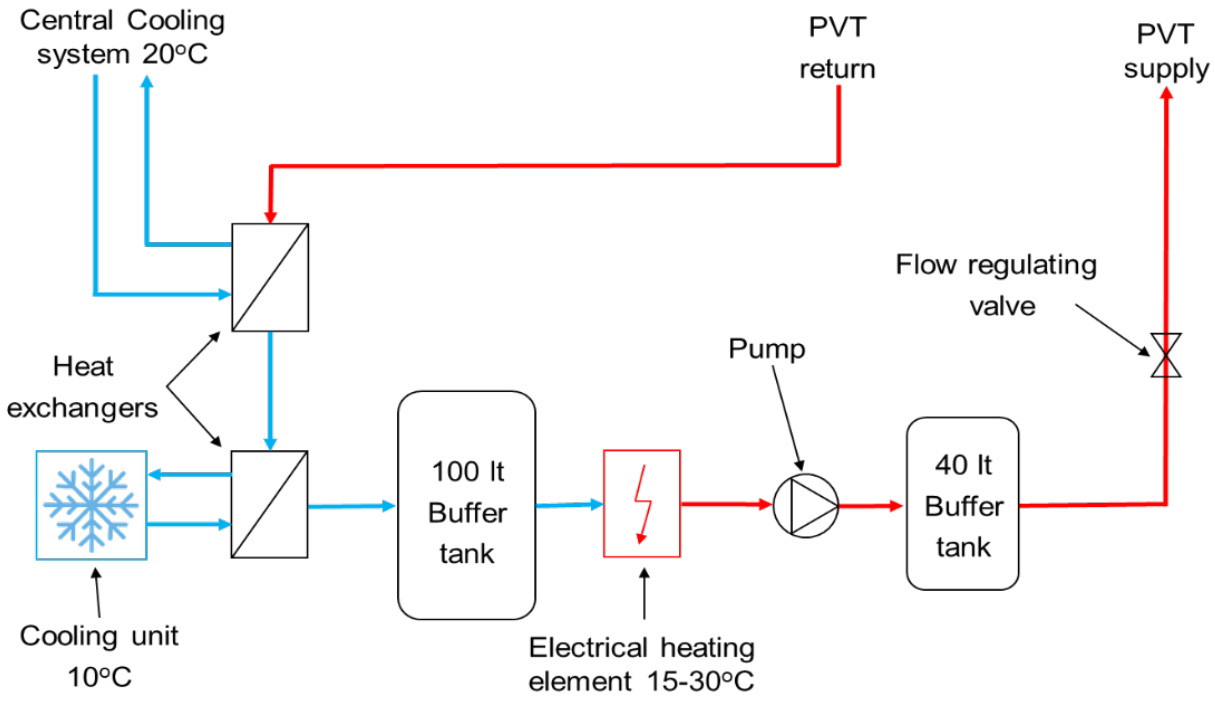

Figure 22. Equipment setup for keeping constant forward temperature.

The electrical output from the PVT panels, the total and long-wave irradiance as well as the ambient temperature were measured. The temperature differences between the inlet and outlet temperatures to and from the thermal absorbers were measured using thermopiles and the volume flow rates through the absorbers were likewise measured. Since it was expected that the wall temperature would affect the thermal performance of the panels, the temperature inside the wall behind the panels was also measured. The wind speed near the PVT panel was measured with an ultrasonic wind sensor mounted in the same plane as the PVT collector as it can be seen in figure 23.

Figure 23. Location of the ultrasonic wind sensor.

The thermal performance of the PVT panel is normally characterized using the quasi-dynamic test (QDT) method as it is described in ISO 9806:2017 (ISO 9806:2017(E), 2017), using the equation:

$$\dot{Q} = A_G\left[\eta_{0,b}K_bG_b + \eta_{0,b}K_dG_d - a_1(T_m - T_{amb}) - a_2(T_m - T_{amb})^2 - a_3u'(T_m - T_{amb}) + a_4(E_L - \sigma T_{amb}^4) - a_5(dT_m/dt) - a_6u'G - a_7u'(E_L - \sigma T_{amb}^4) - a_8(T_m - T_{amb})^4\right]$$

where $u' = u - 3$, α_7 [W m^{-2} K^{-4}] is the wind speed dependence of infrared radiation exchange and α_8 [W m^{-2} K^{-4}] is the radiation losses.

A modified version of the above mentioned equation was used, utilizing the total irradiance on the collector plane and the incidence angle modifier:

$$\dot{Q} = A_G\left[\eta_{0,b}K_\theta G_t - a_1(T_m - T_{amb}) - a_2(T_m - T_{amb})^2 - a_3u'(T_m - T_{amb}) + a_4(E_L - \sigma T_{amb}^4) - a_5(dT_m/dt) - a_6u'G - a_7u'(E_L - \sigma T_{amb}^4) - a_8(T_m - T_{amb})^4\right]$$

$$K_\theta = 1 - b_0\left(\frac{1}{cos\theta_i} - 1\right)$$

The coefficients for the panel performance were calculated at maximum power point tracking (MPPT) operation.

The wall on which the PVT panels are integrated, can be heated up or cooled down by the ambient temperature, the solar irradiance and the panel temperature and this can increase or decrease the efficiency of the PVT. For this reason, it was decided to perform two analyses using the QDT method. The first method applied was the standard QDT formula as presented in the equation above and the second one was an extended version of the QDT equation, where a new term (α_9) was added, which would take into consideration the temperature of the wall T_w compared to the mean temperature of the PVT. The extended QDT equation is presented by:

$$\dot{Q} = A_G\left[\eta_{0,b}K_\theta G_t - a_1(T_m - T_{amb}) - a_2(T_m - T_{amb})^2 - a_3u'(T_m - T_{amb}) + a_4(E_L - \sigma T_{amb}^4) - a_5(dT_m/dt) - a_6u'G - a_7u'(E_L - \sigma T_{amb}^4) - a_8(T_m - T_{amb})^4 - a_9(T_m - T_w)\right]$$

The electrical power produced by the two panels along with the solar irradiance on the panels' surface is illustrated in figure 24 for June 27. It can be observed that the uninsulated panel produced slightly more electricity than the insulated one. This phenomenon was observed for all the measurement days according to table 9. However, it has to be pointed out that the absolute difference of the average daily electrical output of the two panels was only about 0.5%.

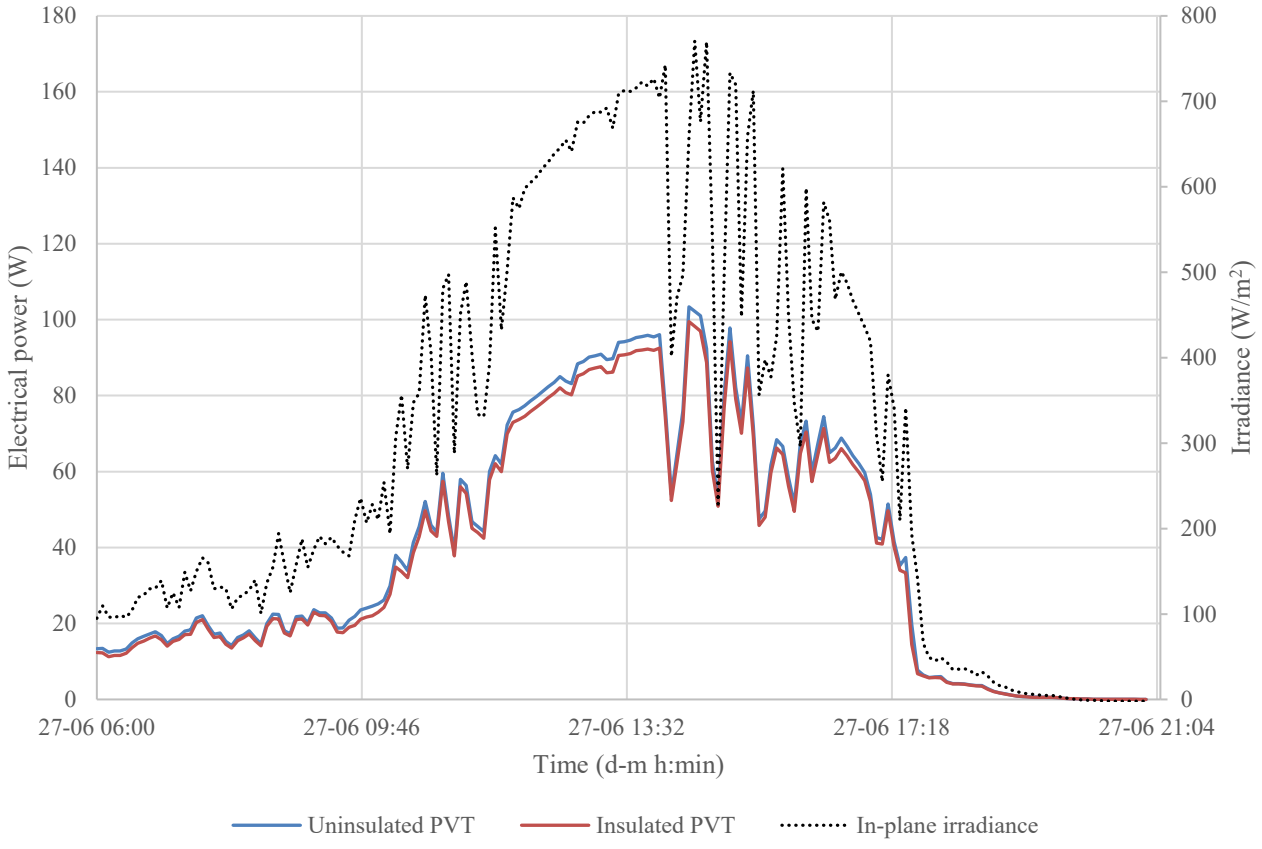

Figure 24. Electrical power and solar irradiance on panels for 27/06/2019.

	Non-insulated panel electrical efficiency (%)	Insulated panel electrical efficiency (%)	Abs. difference (%)
27 – 06 – 2019	13.4	12.9	0.5
03 – 07 – 2019	13.6	13.1	0.5
05 – 07 – 2019	13.4	12.9	0.5
09 – 07 – 2019	13.5	13	0.5
10 – 07 – 2019	13.6	13.1	0.5
11 – 07 – 2019	13.4	12.8	0.6
16 – 07 – 2019	14.1	13.5	0.6
23 – 07 – 2019	13.9	13.3	0.6
28 – 07 – 2019	13.3	12.9	0.4
16 – 08 – 2019	13.9	13.3	0.6

Table 9. Average daily electrical efficiencies.

The reason for this difference in electrical output was the different temperature of each panel. In figure 25, the outlet fluid temperature of the two panels is presented along with the fluid inlet temperature and the irradiance on the panels' surface. The inlet fluid temperature was the same for the two panels. It can be seen that the outlet fluid temperature of the insulated panel is always higher than the uninsulated one, for periods of the day where the panel is heated by the sun. However, in the afternoon, where the irradiance on the panels' surface drops rapidly, it can be seen that the outlet temperature of the uninsulated panel is higher than the insulated one. This phenomenon was observed through all the measurement days with high irradiance.

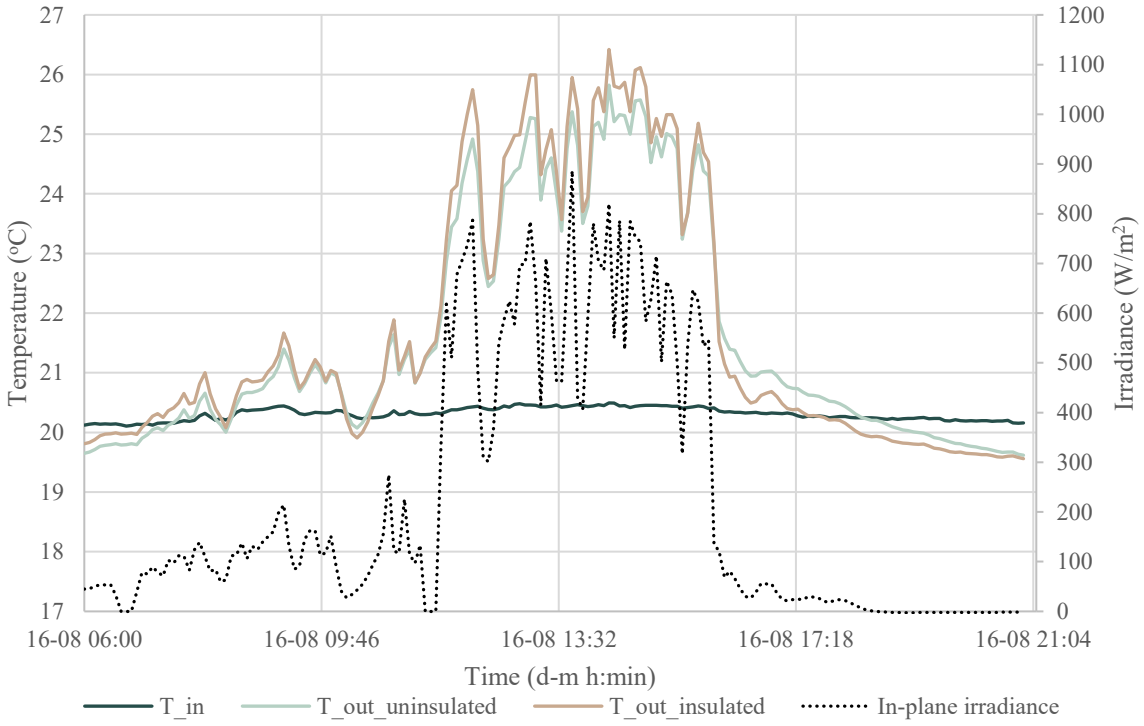

Figure 25. Inlet and outlet fluid temperature and tilted irradiance for 16/08/2019.

A possible explanation of this behavior is given in figure 26 where the wall temperature behind the insulated and the uninsulated panel is presented along with the mean temperature of the two panels. It can be observed that the wall temperature behind the uninsulated panel reached much higher levels, being affected by the mean temperature of the panel and the irradiation. The temperature of the wall varied behind the two panels approximately 2 – 4 K over the day. In the afternoon, the wall discharged its heat to the panel increasing its mean temperature. This effect is much more significant for the uninsulated panel because there is no insulation to reduce the heat transfer, but also because of the higher wall temperature. This behavior was observed for all measurement days with high irradiance.

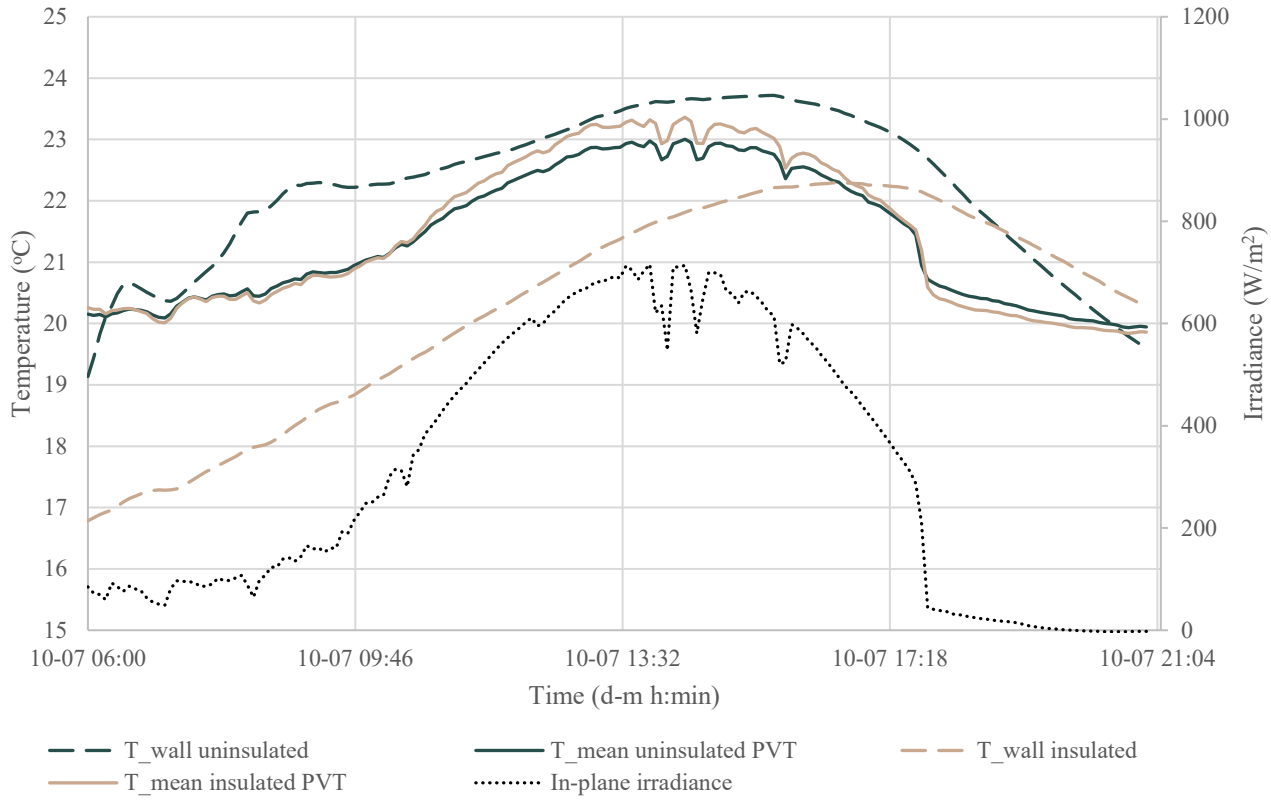

Figure 26. Wall and mean panel temperatures and solar irradiance on panels for 10/07/2019.

Applying the two versions of the QDT equations, the thermal performance of the uninsulated panel was calculated. The calculated thermal output from the standard and the extended QDT is reported in table 10 and the obtained coefficients from the two methods are reported in table 11.

Date	Start time	End time	T_{in} (°C)	Measured thermal output (kWh)	Standard QDT		Extended QDT	
					Modelled thermal output (kWh)	Deviation (%)	Modelled thermal output (kWh)	Deviation (%)
27 – 06	12:00	17:00	30	3.27	2.95	-9.9	3.16	-3.4
03 – 07	12:00	15:00	25	1.96	2	2.3	1.98	1.4
05 – 07	11:00	14:00	25	2.2	2.3	4	2.28	3.1
09 – 07	11:00	16:00	20	4.28	4.21	-1.7	4.5	5
10 – 07	10:00	16:00	20	5.94	5.87	-1.2	5.87	-1.2
11 – 07	10:00	14:00	20	3.95	4.03	1.9	3.98	0.7
16 – 07	11:00	16:30	15	6.78	6.81	0.4	6.87	1.2
23 – 07	10:00	17:00	15	8.79	8.44	-4	8.62	-1.9
28 – 07	12:30	16:00	30	2.74	2.84	3.7	2.66	-2.6
16 – 08	12:00	16:00	20	4.28	4.32	0.9	4.22	-1.5

Table 10. Thermal performance results for uninsulated PVT.

	Standard QDT		Extended QDT	
	Coefficients	t-scores	Coefficients	t-scores
$\eta_{0,b}$ (-)	0.59	24	0.53	27
b_0 (-)	0.12	15	0.14	21
α_1 (W m^{-2} K^{-1})	17.7	68	7.1	12
α_5 (J m^{-2} K^{-1})	4.4 *10^4	32	3.9 *10^4	35
α_6 (m^{-1} s)	0.06	6	0.06	8
α_9 (W m^{-2} K^{-1})	-	-	24.8	20

Table 11. Collector coefficients from quasi-dynamic testing (based on gross area).

Adding the new term in the QDT equation changed all the coefficients calculated from QDT except of the value of α_6. Coefficient α_9 takes into account the heat losses (or heat gains) from the panel to the wall and seems to be very significant from a statistical point of view (high t-score). This new coefficient leads to a reduction of α_1, which is due to the fact that the heat losses to the wall are taken into account by coefficient α_9. The decrease of coefficient α_5 was not anticipated and is thought to be caused by the interplay of the thermal mass of the wall and is changed due to the addition of coefficient α_9. In theory, the introduction of coefficient α_9 should not have any effect on the $\eta_{0,b}$ and b_0 coefficients. However, both coefficients changed with the introduction of the new factor. It is not clear if the standard or the extended formula calculates more accurately the results and more investigations have to be conducted. It has to be pointed out though that the deviation of the daily calculated values for the extended formula of QDT are smaller, suggesting that, in general, it calculates more accurately the thermal performance of the panel. The suggested extended version of QDT was also applied to the insulated panel. In that case, the t-score of α_9 coefficient was below 3, so it was considered insignificant, proving that, in the case of the insulated panel, the wall temperature does not affect the thermal performance. This result enhances the belief that the addition of α_9 coefficient was necessary in the QDT formula.

In this study, two façade integrated PVT panels were investigated in terms of thermal performance. One of them had a layer of insulation between the panel and the wall and the other was in direct contact with the wall. It was found that the insulated panel had higher thermal performance than the uninsulated one, as higher

outlet fluid temperatures were reached. On the other hand, due to lower temperature of the panel, the uninsulated one had higher electrical performance. It was pointed out that the wall affected significantly the thermal performance of the panel, especially of the uninsulated panel, since it created additional heat losses or heat gains to the panel. For this reason, a new factor was suggested to be used in the standard QDT formula that takes into account the wall temperature. The obtained results for this new coefficient justified this addition, showing a considerable statistical importance of the new coefficient. It has to be mentioned that for the insulated panel the new coefficient was statistical insignificant as was to be expected. However, although the extended QDT formula showed promising results in term of modelling of thermal performance of the panel, more investigations are considered necessary in order to reach a final conclusion on whether this factor should be added to the standard QDT formula.

5.5 Analyses of operation of full scale PVT systems

Measurements for a PVT/heat pump system installed in Ølstylkke in 2018 consisting of 35 m² roof integrated PVT panels, a modulating 3-12 kW Danfoss Varius Pro+ heat pump and a 7.5 kWh Fronius battery have been analysed. Figure 27 shows a photo and a principle sketch of the system. The system, which supplies all space heating and domestic hot water to the house, also included 60 m² PV panels on the north-facing roof. The heat pump is located in the depository attached to the northern wall of the house.

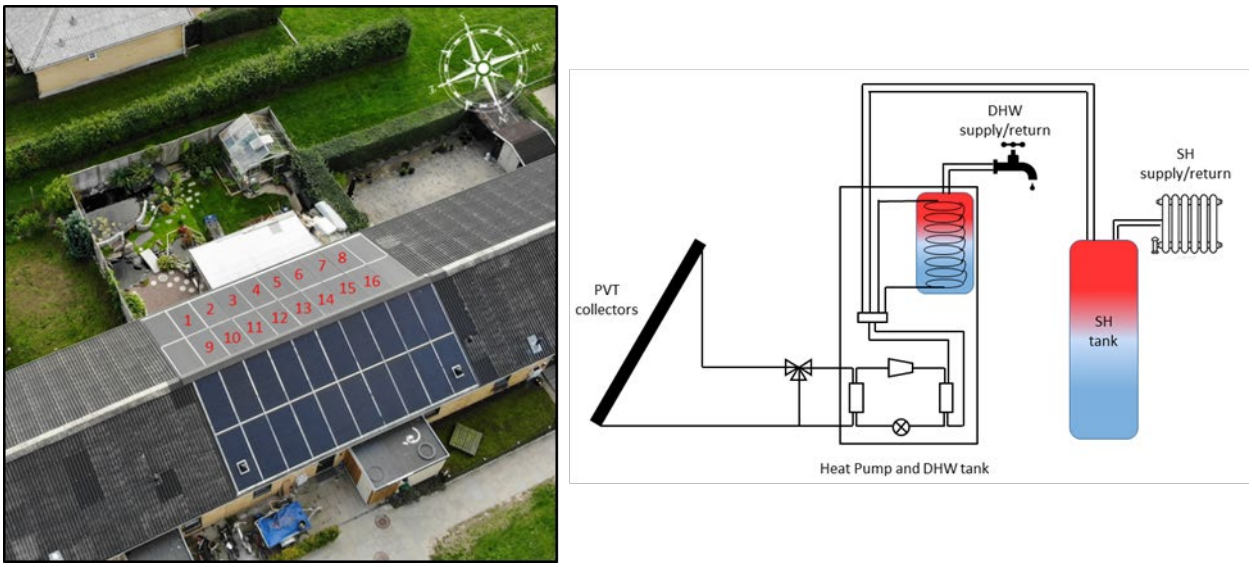

Figure 27. Aerial photo of the roof integrated PVT panels and schematic sketch of the system.

The PVT panels produces both heat and electricity and the heat is both produced by solar radiation and by the ambient air.

Measurements of the space heating demand and the hot water consumption of the house were carried out. The electricity consumption of the heat pump, the heat production of the PVT panels, the electricity production of the PVT and PV panels and weather data such as solar radiation on the PVT panels and the outdoor temperature were measured. By means of the measurements, it is possible to determine the efficiency of the heat pump.

In figure 28 daily measured space heating demands are shown with orange color and daily hot water consumptions are shown with blue color for a measuring year. The heat demand is very small compared to the size of the heat pump. The highest average daily space heating demand is lower than 2 kW, while the lowest power of the heat pump is 3 kW. The heat pump is therefore strongly oversized. This results in relatively short

operation periods of the heat pump and relatively low heat pump efficiency. It should be noted that heat pumps of the right small size are not available on the marked.

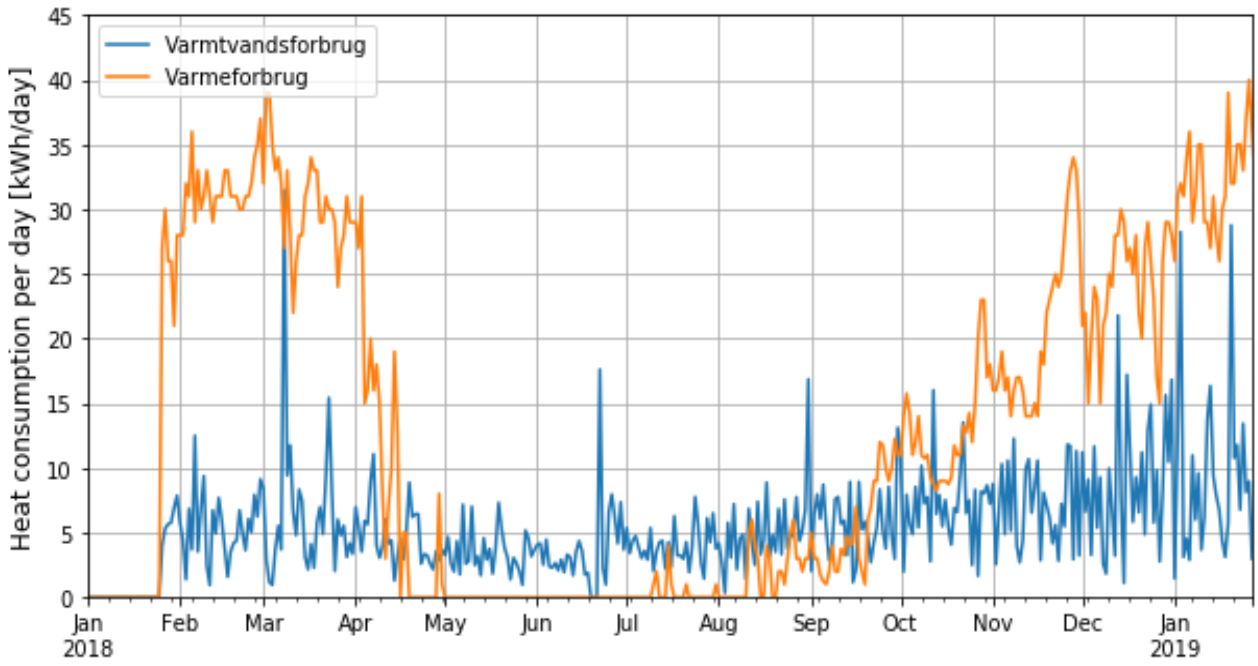

Figure 28. Measured daily space heating demand and domestic hot water consumption.

Figure 29 shows measured (blue dots) and corrected (orange dots) daily COP values for the heat pump as a function of the outdoor temperature. The measured values are the ratios between the space heating demand plus the domestic hot water consumption and the electricity consumption of the heat pump. The corrected values include the estimated heat loss of the depository where the heat pump is located. The COP values are increasing for increasing outdoor temperature. The COP values are relatively low, both due to the oversized heat pump and due to a high heat loss from the heat pump, the pipes and the tanks. It is nevertheless estimated, that the heat pump is working in a reasonable way. The system is able to heat the house during all days of the year.

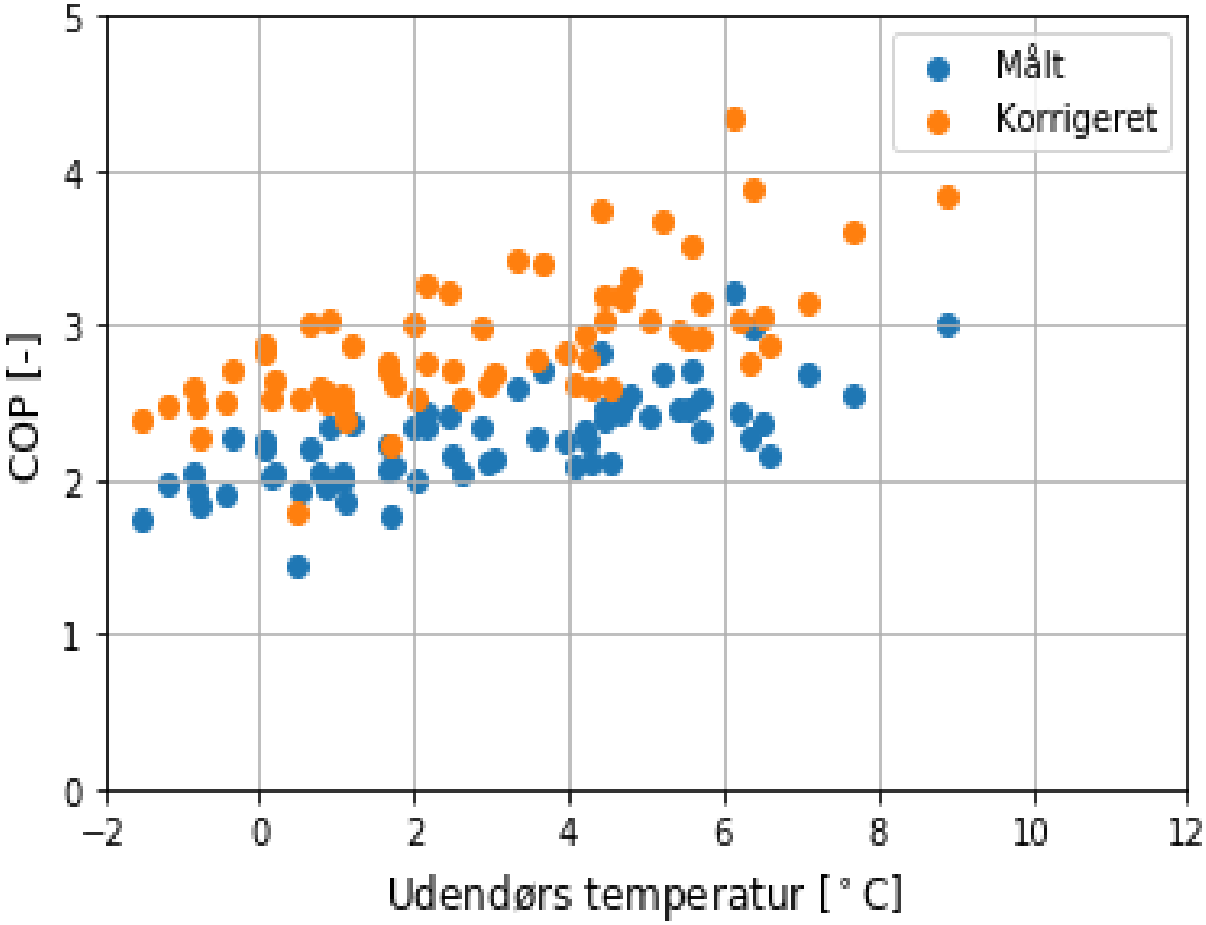

Figure 29. Measured and corrected daily COP values for the heat pump as function of the average daily outdoor temperature.

The daily electricity productions of the PVT panels and the PV panels are shown in figure 30 for April 1. – April 25., 2019. The electricity quantities delivered to the grid, to the battery and the electricity directly used in the house are shown. It must be mentioned, that the battery was first put in operation April 11. It is estimated, that the performance and operation is reasonable, also from an electricity point of view.

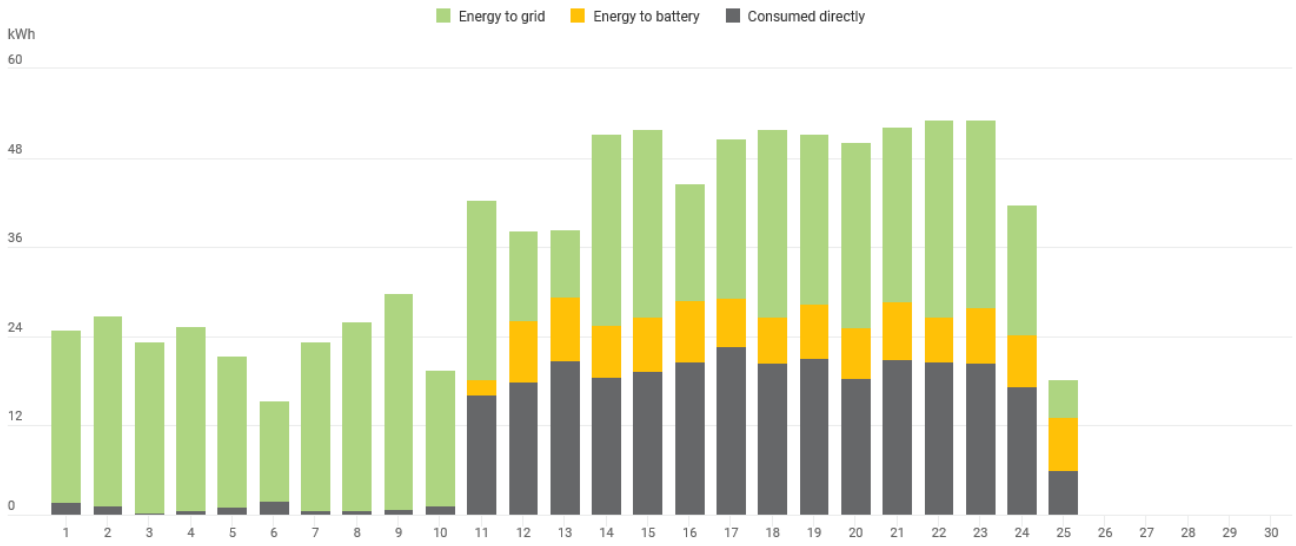

Figure 30. Daily energy quantities from PV and PVT panels to grid, battery and direct consumption for April 2019.

A few times during cold periods in the winter, the control system of the heat pump automatically stopped the operation of the heat pump due to a too low temperature of about -10°C in the PVT loop. In these periods an electric heating element covers the heat demand. It occurs during periods with a clear sky and a low ambient temperature. The oversizing of the heat pump contributes to this problem, since the heat transfer fluid is cooled down by the heat pump with a high power. The control of the system must be improved so that the heat pump is not stopped during cold periods. It is estimated, that the yearly performance of the system is not strongly influenced by the few periods with these control problems.

All in all the system works as planned, and there are many possibilities for smart control strategies for the system. The system can with the battery and the heat storage be operated in a way so the system has a good interplay with the energy system.

A simulation model of the system was developed in the simulation software TRNSYS, http://www.trnsys.com/. The model was validated with measurements for a period of two weeks, from 14/2/2019 to 28/2/2019.

The equation used for modelling the thermal output of the PVT panels was:

$$\dot{Q} = A\,[\eta_0 K_\theta G_t - a_1(T_m - T_{amb}) - a_5(dT_m/dt)]$$

where A_G is the gross area of the panels, η_0 the peak collector efficiency, K_θ the incidence angle modifier, G_t the total irradiance on the panel plane, α_1 the heat loss coefficient, α_5 the effective thermal capacity, T_m the mean fluid panel temperature and T_{amb} the ambient temperature.

The equation used for modelling the electrical output of the PVT panel was:

$$P_{el} = \eta_{el,ref} \cdot G_t \cdot A_{PV} \cdot PR_{IAM} \cdot PR_T \cdot PR_G$$

where $\eta_{el,ref}$ is the electrical efficiency at reference conditions, G_t is the total irradiance on the panel plane, A_{PV} is the area of the PV area, PR_{IAM} is the loss effects of incidence angle, PR_T is the temperature dependence of the electrical efficiency and PR_G is the loss effects of irradiance.

The parameters used for the simulations are given in table 12.

Parameter	Value	Unit
Optical efficiency	0.6	-
Linear heat loss coefficient	20	W/m^2K
Effective thermal capacity	15	kJ/m^2K
Incidence angle modifier (b0)	0.09	-
Electrical efficiency at reference conditions	0.18	-
Temperature coefficient of solar cell efficiency	-0.4	%/K
Irradiance dependence of PV efficiency	-0.00045	W/m^2K

Table 12. Parameters used for modelling of the PVT panel.

Energy quantities of the system and COP of the heat pump calculated with the TRNSYS model are compared to measurements from the system in figure 31. There is generally a good match between the compared quantities. The difference between the measured and modelled values for the simulated period was around 2% for all of the investigated quantities. The corresponding bias for each quantity are presented in table 13. Based on the investigations it is judged that the model is validated and that it can be used for calculations aimed to optimize the system design.

Parameter	Bias [%]
PVT collector thermal output	2.1
PVT collector electrical output	-2.1
Heat pump COP	2.2
DHW energy consumption	-2.3
SH energy consumption	-2.3

Table 13. Variation between the measured and the simulated parameters for the investigated period.

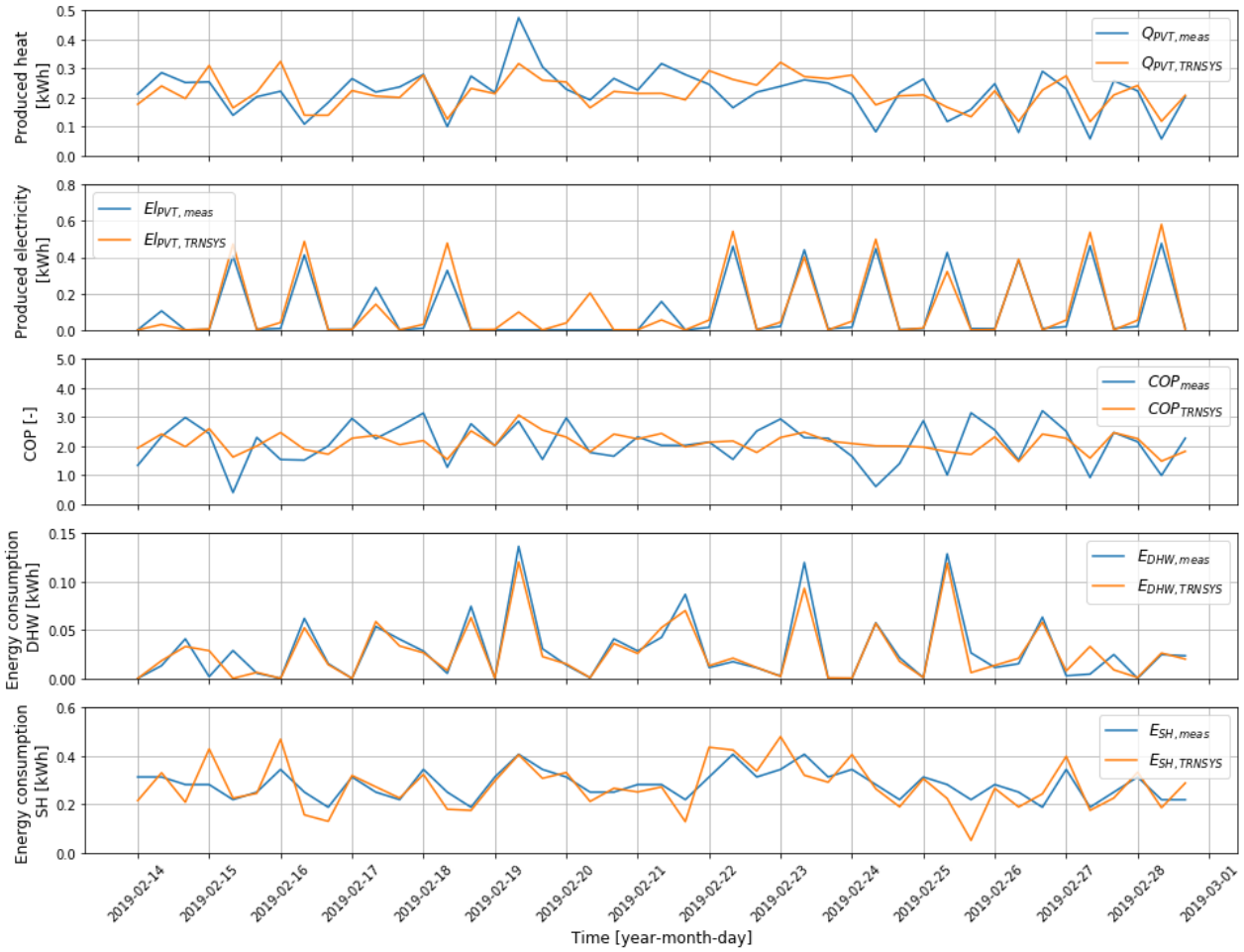

Figure 31. Comparison of measurements from the pilot system and modelled values from the TRNSYS simulation.

With the validated TRNSYS model calculations of the yearly performance of the system were carried out with weather data from the Danish Reference Year. The results are shown in figure 32.

The heat load during the non-heating period only consisting of domestic hot water consumption is very small. This results in sporadic operation of the heat pump and thus very little heat from the PVT panel utilized. However, the increased temperature of the brine entering the source of the heat pump increased marginally the COP during the summer period. The daily mean COP of the heat pump is 3.5 during the summer. The yearly mean COP of the heat pump is 3.15. The developed simulation model is suitable in connection with planning and optimization of future PVT/heat pump systems.

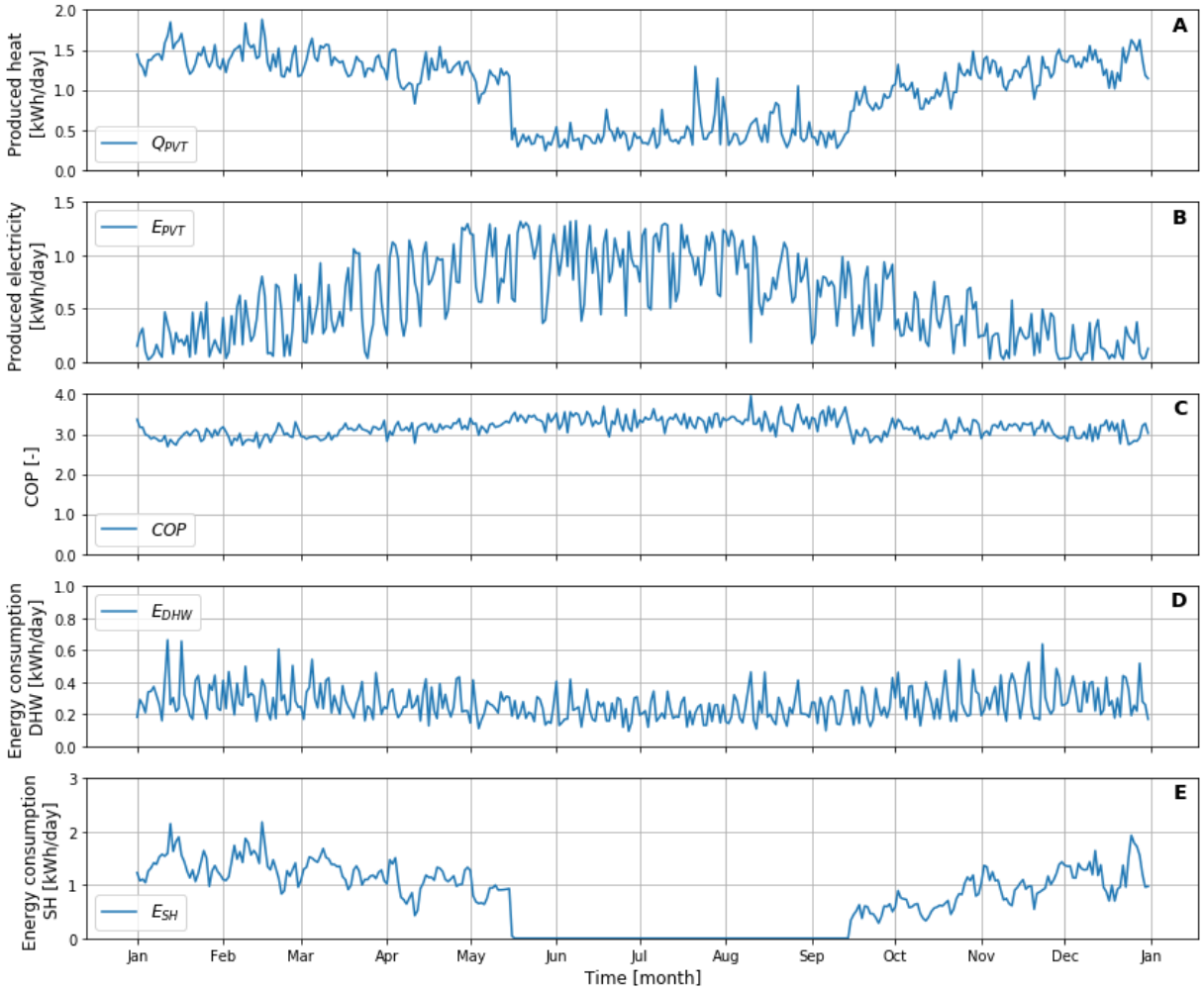

Figure 32. Mean daily values for Q_{PVT}, E_{PVT}, COP, E_{DHW} and E_{SH} from the yearly simulation of the system.

A PVT/heat pump system installed at a football club house in Stenløse was used as study case for the IEA Task 60 project, https://task60.iea-shc.org/.

A 25 kW ground source heat pump and 24 PVT panels (Racell SE1100-220 Hercules iTM) were installed as a new roof of the building (total panel area, 165 m^2; 24.6 kWp electrical output). The modules are oriented to the south with a tilt angle of 25°. In addition, a PV system with the opposite orientation (North) comprising 24 modules of the same type, though without heat absorbers, was installed (165 m^2; 24.6 kWp). Figure 33 shows the south-facing PVT roof.

The heat supply system is depicted in a simplified form in figure 34. The heat pump is coupled with 1500 m horizontal pipes. The heat is delivered to the 850 l buffer tank in 2 different levels – low- and mid temperatures normally up to 55°C - and high temperature from the super heater part up to 65°C. The buffer tank supplies high temperature heat to the domestic hot water tank and to the central heating system by 25-55°C.

The PVT delivers heat to the buffer tank through an integrated heating coil. On warm summerdays the buffer tank is heated up to more than 60°C. In cooler periods with lower PVT temperatures the heat can be supplied to the ground source pipes to be stored there and used later by the heat pump.

Figure 33. View of the PVT system integrated in the roof of the football club house in Stenløse.

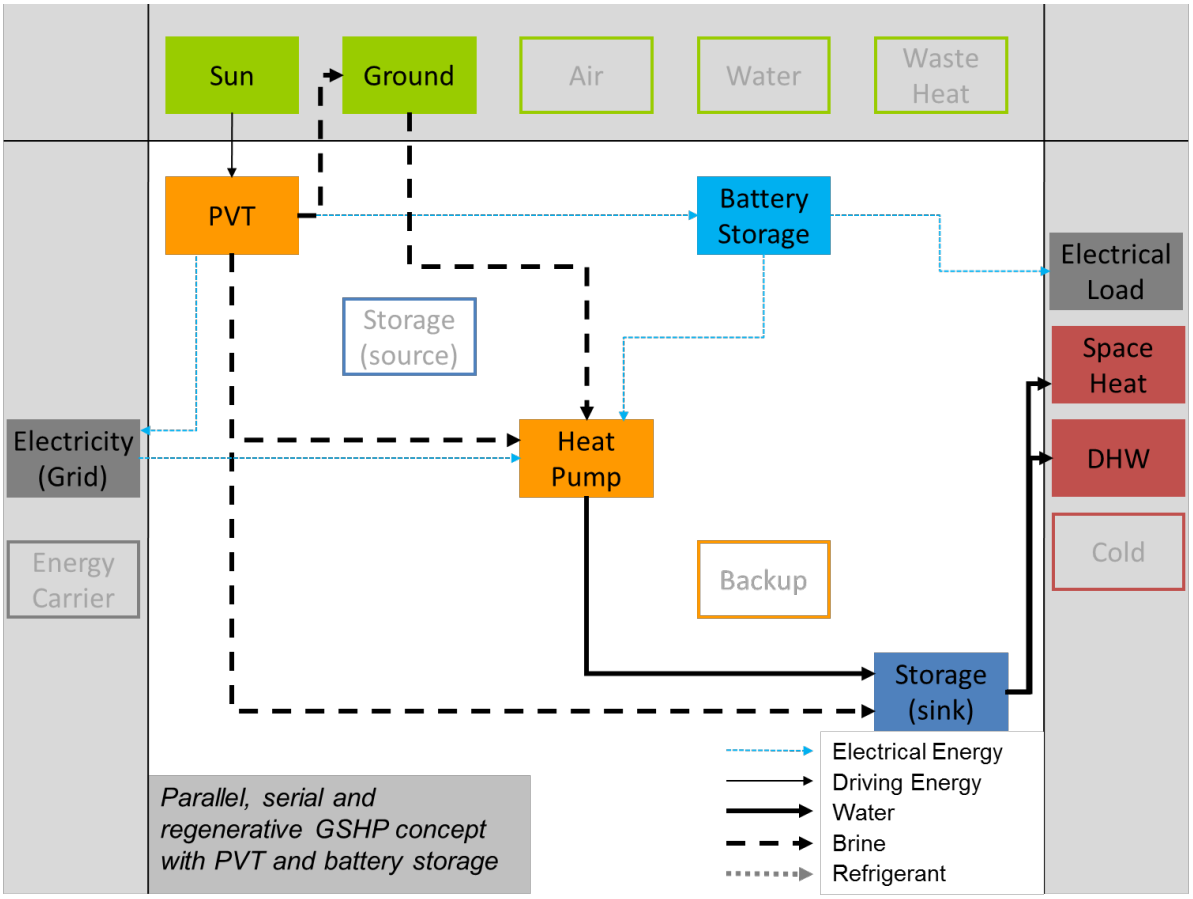

Figure 34. Schematic principle of PVT system in Stenløse.

Another example of a PVT system is the system at Egeris Sports Center in Skive, established in 2013, see figure 35.

Figure 35. PVT system at Egeris Sports Center in Skive.

The system has 42 PVT modules installed on top of a roof facing south. The 2m x 3.2m modules have no rear or front insulation and are 7 mm thick with 4 mm front glass. Each module weighs 70 kg.

The electrical energy runs all the facilities in the building and the thermal energy provides domestic hot water for the many showers provided for the sports athletes. Mainly football is exercised having several football fields outside, see figure 36.

Figure 36. Aerial photo of Egeris Sports Center with PVT panels

The building has 12 locker rooms, offices, meeting rooms, depots and a canteen.

Each module has 228 mono-Xtal cells and electrical energy of 1025 Wp at STC. There are no Junction boxes, but instead 456 bypass diodes are integrated directly with the cells, thus minimizing hotspots and shading effects. The module energy absorber is able to deliver 2000 W of thermal power at peak condition.

The thermal header pipes of the MPE aluminium absorbers are connected in parallel, thus minimizing temperature gradients across the series connected solar cells.

5.6 Dissemination

The project results were disseminated by participation in the following expert meetings of the IEA Task 16 project:

- Participation in expert meeting in March 2018 in Freiburg, Germany.
- Participation in expert meeting in October 2018 in Zaragoza, Spain.
- Participation in expert meeting in May 2019 in Eindhoven, the Netherlands.
- Participation in expert meeting in October 2019 in Kgs. Lyngby, Denmark.
- Participation in online expert meeting in April 2020.
- Participation in online expert meeting in October 2020.

Further, project results were disseminated by participation at the following conferences and meetings:

- Presentation of Experimental investigation and characterization of façade integrated PVT collectors with and without insulation at ISES Solar World Congress 2019, Santiago, Chile.
- Industry workshop in October 2019 at the Technical University of Denmark for the Danish solar industry with the following presentations: Introduction IEA SHC Task 60 on PVT systems by Jean-Christophe Hadorn, Switzerland, PVT market analysis for Solar Heat Worldwide by Thomas Ramschak, AEE, Austria, PVT collector test standards by Korbinian Kramer, Fraunhofer ISE, Germany, PVT architecture and good examples by Lars Erik Bancroft, Arkitema Architects, Denmark, Market potential for PVT by Svend Erik Mikkelsen, COWI, Denmark, Case study of BIPVT by Niels Radisch, Rambøll, Denmark, Key findings in system simulations of PVT system by Mark Dannemand, DTU Civil Engineering, Denmark, Smart control of energy systems with PVT by Peder Bacher, DTU COMPUTE, Denmark and presentation of the PVT collector manufacturers Abora (Spain), Sunovate (Australia), Naked Energy (UK) and Dual Sun (France).
- The Green and Circular Economy - dynamics and governance Leadership course (GCE-L). Leadership course under the DFC Scholarship Programme, December 2019. The PVT-E concept, markets and impact. Specific examples for full scale systems and simulation results for large scale buildings. Participants: top leaders mainly from Indonesia, Kenya and Denmark, working to enhance a green and/or circular economy, representing different stakeholders in each country from e.g. ministries of environment, industry and planning, local authorities, utilities and business organizations.
- CLEAN Cluster seminar: Connecting Zealand med Korsør Havn - udvikling i virksomheder, der arbejder med miljøteknologi eller har fokus på ressourceeffektivitet, March 2019. Participants: 25 Danish companies, Korsør Harbour management. Presentation of how PVT-E systems work and focus on CHP Cooling.
- ONE-STOP-SHOP workshop by Municipality of Copenhagen: PV & PVT for residential building blox in urban areas, May 2019. Participants: 15 boards of housing companies and residential building box in Copenhagen.

Project results were also disseminated by publications of papers in scientific journals and reports:

- Dannemand M., Perers B. & Furbo S. (2019). Performance of a demonstration solar PVT assisted heat pump system with cold buffer storage and domestic hot water storage tanks. Energy & Buildings Volume 188, pp. 46–57.
- Dannemand M., Sifnaios I, Zhiyong T. & Furbo S. (2020). Simulation and optimization of a hybrid unglazed solar photovoltaicthermal collector and heat pump system with two storage tanks. Energy Conversion and Management Volume 206, article 112429.

Students following solar energy courses at the Technical University of Denmark have been informed about the project results.

Finally, information on the IEA Task 60 project is available on the homepage: https://task60.iea-shc.org/

6. Utilisation of project results

RACELL will utilize the project results in their efforts to increase the market for PVT systems and in connection with their development work on improved PVT panels and PVT systems. The applications for PVT in urban areas have shown to be manifold and from the project results they are including the facades, no matter shading, since the absorbers of unglazed PVT are also active in dark and during the night hours. Thus owners of large scale buildings will be utilizing the technology.

As the PVT also benefits from the architectural designs available for PV, it is assumed that commercialization will be done together with well-known architect companies. Direct approach and seminars for international entrepreneur firms will also be an important approach for commercializing the projects. In all cases studies as elaborated in this project are most valuable, because building owners and entrepreneurs demand safe references of these new technology solutions.

The results have been opening up for concrete project proposals for building projects in Scandinavia, Philippines and Australia. Also, well-known investors have approached the production company and we expect some major upgrading and automation of the production line by these investments. The point is that a large production capacity is needed for the promising large-scale projects.

Competition is high in the building industry and well described products and solutions are the key for getting a fast route into this industry. Because PVT is a new product, the markets tend to be conservative and choose the cheapest and best-known products, which are standard PV modules. Therefore, it is of utmost importance to have the complete financial package including ROI, DGNB benefits, mounting costs, maintenance, energy cost savings, dependence upon energy sale tariffs etc. along hand in hand with the technology. Request for product certificates and data sheets, which internationally are still well defined, are a must and thus creates a marketing barrier.

In general, once the references have been established, and the product and technology has become a stanard in the building industry, the PVT market will grow exponentially and create hundreds of jobs in Denmark and thousands internationally.

The project results are useful for manufacturers of solar collectors, PV panels and PVT panels in connection with their efforts to improve their products. The project results are also useful for consultants and planners aiming to improve marketed solar energy systems. Further, the project results are useful for solar energy researchers aiming to determine optimal solar energy systems for the future. Overall, the project results form an excellent basis for future development of solar energy solutions.

The project contributes to improved solar energy solutions for the future. Therefore, the project contributes to a future sustainable energy system.

The project results have been presented for students following courses at the Technical University of Denmark.

7. Project conclusion and perspective

The project resulted through participation in the IEA Task 60 project in an overview of the possibilities of using PVT panels in systems with other components and in optimized designs of PVT systems for different applications. Further, different PVT panels were by means of experimental investigations characterized by determining efficiency expressions, so that the performances of PVT panels can be calculated for all weather conditions and temperature levels. Furthermore, simulation models of PVT systems based on the efficiency expressions were developed. These simulation models are useful in connection development of improved PVT systems in the future.

Based on the project results improved PVT panels and PVT systems can be developed. Consequently, the project results are valuable for the solar energy industry in connection with their efforts to develop, design and optimize their solar energy systems in the best possible way. The results are also valuable for consultants in connection with planning of PVT systems.

8. Appendices

Dannemand M., Perers B. & Furbo S. (2019). Performance of a demonstration solar PVT assisted heat pump system with cold buffer storage and domestic hot water storage tanks. Energy & Buildings Volume 188, pp. 46–57.

Dannemand M., Sifnaios I., Jensen A.R. & Furbo S. (2019). Experimental investigation and characterization of façade integrated PVT collectors with and without insulation. ISES Solar World Congress 2019, Santiago, Chile.

Dannemand M., Sifnaios I, Zhiyong T. & Furbo S. (2020). Simulation and optimization of a hybrid unglazed solar photovoltaicthermal collector and heat pump system with two storage tanks. Energy Conversion and Management Volume 206, article 112429.

TRNSYS- Transient System Simulation Tool 2019, http://www.trnsys.com/

IEA Task 60 homepage: https://task60.iea-shc.org/